DAM REOPERATION AS AN ADAPTATION STRATEGY FOR SHIFTING PATTERNS OF WATER SUPPLY AND DEMAND

A case study for the Xin’anjiang-Fuchunjiang reservoir cascade, China

Erwin Vonk

UNIVERSITY OF TWENTE.

Master's Thesis

DAM REOPERATION AS AN ADAPTATION STRATEGY FOR SHIFTING PATTERNS OF WATER SUPPLY AND DEMAND

A case study for the Xin'anjiang-Fuchunjiang reservoir cascade, China

Erwin Vonk

BSc., Civil Engineering (University of Twente, Enschede)

In partial fulfillment of the requirements
for the degree of

Master of Science in Civil Engineering and Management

University of Twente

April 16, 2013

Under supervision of the following committee:

Dr. ir. D.C.M. Augustijn
University of Twente, Department of Water Engineering and Management

Dr. ir. M.J. Booij
University of Twente, Department of Water Engineering and Management

Dr. Y. Xu
Zhejiang University, Institute of Hydrology and Water Resources

Abstract

Climate change, rapid economic developments and further growth of the human population are regarded as the major drivers of increasing water-related problems worldwide. The changing hydrological circumstances and water demand patterns pose a challenge to the management of water resources systems as these systems are designed to maintain a fragile balance between water supply and demand. With the projected changes, this balance is likely to be disrupted, ultimately requiring adaptation of the existing infrastructure. In many water resources systems reservoirs are the key element to ensure a stable water supply. Yet, since reservoirs can be characterized as rather inflexible types of infrastructure, one of the few options for adaptation is to adjust their operation. It is however unclear to which degree of water supply and demand changes this so called dam reoperation is still possible.

The objective of this thesis is to determine whether reoperation of the Xin'anjiang-Fuchunjiang reservoir cascade (Hangzhou Region, China) is an effective adaptation strategy to mitigate potential impacts of climate change and regional socio-economic developments. We follow a scenario-based approach to explore the effects of various likely degrees of supply and demand changes for the future period between 2011 and 2040. The outcomes are compared to the control period 1971-2000. Population growth, increasing industrial production and changing land use are considered as driving forces for increasing water demand, while climate change is investigated as process influencing water supply. The scenario-wise changes in water supply and demand are used as forcing for the WEAP water allocation model, which is employed to simulate reservoir performance. This performance is measured using the Shortage Index (SI) as indicator for water shortages and the Mean Annual Energy Production (MAEP) for hydropower generation.

The impact of climate change and socio-economic developments on the reservoir system is determined by simulating the performance of conventional operating rules for both the control period and each future scenario. We find a SI of 0.007 for the control period and values ranging from 0.05 to 0.92 for the investigated future scenarios. The largest annual deficit is 3.9 billion m^3 (15% of the annual supply requirement), simulated in the high water stress scenario. Even though the increasing SI implies that more drought problems are likely in the future period, the deficits are still fairly small compared to what is generally regarded acceptable in the literature. Next to the increasing water shortages, simulation of the various scenarios shows a decrease between -12.8% and -16.3% for the MAEP.

In a second step the water allocation model is interlinked with the NSGA-II metaheuristic algorithm in order to derive long-term multireservoir operating rules adapted to each scenario. Based on the optimization results, we conclude that for this case dam reoperation is an effective adaptation strategy to reduce the impact of changing patterns of water supply and demand. Compared to conventional operation, operating rules that are adapted to the forecasted changes can reduce the SI with approximately 72% while the MAEP shows an average increase of 5.4%. Due to the fact that the average inflow in all scenarios is lower than during the control period, adapted operating rules cannot completely restore the system performance to that of the control period. The performance gains for energy production are thus limited to avoiding unnecessary spills and maintaining an optimal head over the turbines.

Preface

In this Master's Thesis my findings of about six months research are presented. The aim of this research project was to investigate the effects of climate change and socio-economic developments on the performance of a reservoir cascade in the Qiantang River Basin and to determine whether the negative impacts can be mitigated by dam reoperation. Answering the research questions required extensive data collection, appropriate implementation of the relevant aspects in a water allocation model and the optimization of reservoir operating rules using a metaheuristic algorithm.

The project was conducted at the Water Engineering and Management department of the University of Twente and partially at the Institute of Hydrology and Water Resources of Zhejiang University (Hangzhou, China). In close cooperation with the researchers in China I collected the data required as input for the water allocation model. I would like to thank my colleagues Zhang Xujie, Zhu Qian and Ma Chong for their help in searching and translating loads of data from various design reports and for their great work on the setup of the hydrological models and evaluation of the climate change scenarios. I also want to mention Tian Ye and thank her for her useful advice on bias correction techniques.

During this research project I was supervised by Denie Augustijn, Martijn Booij and Yueping Xu. I want to express my sincere gratitude to all of them, as they have put a lot of effort in making it all possible. Yueping did a fantastic job in arranging all the required data and facilitating my stay in Hangzhou, while Martijn and Denie have given me a lot of useful feedback on my reports.

Finally there are my office mates, both in China and the Netherlands, with whom I absolutely had a fantastic time. I will always remember the many pingpong tournaments, hiking trips, dinners and karaoke sessions with my friends and colleagues in the Anzhong building and the fun moments with my fellow students in Enschede. The Master's Thesis however not only marks the end this single research project, it is also the closure of many years education. It are my parents Jelle and Wietske that have ultimately made all of this possible and whom I want to thank for their everlasting support and encouragement.

Erwin Vonk
Enschede, April 2013

Contents

Glossary

Active storage zone - Middle reservoir storage zone, between spillway crest level and the Minimum Drawdown Level (MDDL). Also named conservation pool.

Agricultural water demand - Water required for agricultural purposes, including irrigation, drinking water for livestock and water to fill fishing ponds.

Base load plant - Type of power plant that operates continuously, thereby supplying a constant base load to the electricity grid.

Capacity ratio - Reservoir active storage capacity relative to the mean annual inflow.

Cash crop - Crop type grown for sale. Crop types within this category typically have relatively high profit margins and are often exported to other countries.

Chromosome - The data structure of an individual, in which all decision variables are coded in the form of a fixed-length vector.

Conservation pool - See active storage zone.

Crossover - Operator within a genetic algorithm in which the chromosomes of two parent solutions are swapped, thereby producing a new individual (the child solution).

Dead storage - Reservoir storage zone below bottom outlets. Intended for sediment accumulation.

Deficit event - Period in which continuous water shortages occur.

Domestic water demand - Household water demand.

Firm power - Amount of power that is guaranteed to be generated by the hydropower plant continuously (uninterruptible). Also called base load.

Flood control zone - Highest reservoir storage zone, intended for flood control.

Flushing - Sediment management technique in which sediments are discharged through bottom outlets of the dam at a low pool level.

Freeboard - Vertical distance between Maximum Water Level and the crest of the dam.

Generation - One cycle within the optimization procedure (also referring to the individuals within this cycle).

Hangzhou Region - Sub-provincial city Hangzhou.

Hedging - Operational rules that guide the rationing of water in case of shortages.

Inactive storage zone - All storage beneath the minimum drawdown level, including buffer storage and dead storage.

Individual - Candidate solution during the optimization procedure of a genetic algorithm.

Industrial output - Portion of the Gross Domestic Product that is generated by the secondary sector of the economy.

Industrial water demand - Water required for industrial processes, also including cooling water for power plants.

Installed capacity - Technical upper limit to the output of a power plant. Also referred to as nameplate capacity or plant capacity.

Load-following plant - A type of power plant that is being dispatched as electricity is needed, therefore usually only operating during the peak demand hours of a day.

Metaheuristic algorithm - Computational method used to optimize a problem by improving a random candidate solution iteratively until a satisfactory result is obtained.

Minimum drawdown level - Water level below which the reservoir will not be drawn under normal operation so that the minimum head required for hydropower generation can be maintained.

Multireservoir system - System of interconnected reservoirs in a river. Can be organized either parallel or in series (the latter being referred to as a 'cascade').

Municipal demand - Water requirements of the tertiary and quaternary sector of the economy. Commercial services for example include shops, department stores and hotels. Relevant water-consuming public services are hospitals, offices and schools.

Mutation - Type of operator used in genetic algorithms. As the name suggests, this involves random tweaks to the chromosomes of individuals.

Nameplate capacity - Same as installed capacity.

Pareto front - Set of solutions that are Pareto optimal. Any individual along the Pareto-front can not be improved for a certain criterion without reducing its performance on another criterion.

Penstock - Tunnel through which water is transported from the reservoir to the turbines.

Plant factor - The fraction of each timestep that water is being released while the power plant is online.

Plant load factor - Measure of power plant use, defined as the ratio between average power load on the plant for a certain period divided by the installed capacity.

Pool level - Water level in a reservoir.

Population - The complete set of candidate solutions during the optimization procedure of a genetic algorithm.

Reservoir - Artificial lake (usually the impoundment of a dam).

Reliability - Probability that the reservoir is not in deficit mode.

Rule curve - Visual representation of long-term release rules.

Run-Of-River hydroelectricity - Type of hydropower development in which little or no storage is required to produce energy.

Secondary power - All additional power that is produced above contracted firm power level.

Sluicing - Operational technique in which sediment-laden flood flows are allowed to pass through reservoirs as quickly as possible to prevent deposition in the reservoir.

Solution diversity - Spreading of individual solutions along the Pareto front.

Spillway - Common feature of dams which is used to discharge (spill) water from the reservoir.

Staple crop - Category of crop types that are used to produce the dominant portion of a standard food diet in a given population. Staple crops are different in each country, but the most well known are cereals such as wheat, rice, maize, wheat and potatoes.

Tailwater level - Water level directly downstream of the dam.

Vulnerability - Probabilistic measure indicating the distance between the target releases and the actual releasing during a deficit event.

Chapter 1

Introduction

This chapter addresses the outline of the research project. First the context of the problem is discussed from a broad point of view in Section 1.1. Using this overall perspective as a starting point for reasoning, Section 1.2 outlines the more narrow scope of this thesis. We investigate the Xin'anjiang-Fuchunjiang reservoir cascade as a specific case. This reservoir cascade, situated in *Hangzhou Region* (China), is introduced in Section 1.3. Section 1.4 presents the objective and the main research questions of this study, followed by a brief explanation of the structure of this thesis in Section 1.5.

1.1 Background

Water availability is expected to become one of the pressing global issues of the 21st century. Climate change, rapid economic developments and further growth of the human population are regarded as the major drivers of increasing water-related problems worldwide. According to the Intergovernmental Panel on Climate Change (IPCC, 2007), changes in climate variables such as precipitation and temperature will influence the hydrology of many river basins. A severe impact on water supply, flood risk, irrigation and hydropower production is expected at various levels. Yet a spatial analysis of Vörösmarty et al. (2000) revealed that on a global scale population growth may even have a larger impact on future water scarcity than climate change.

The changing hydrological circumstances and water demand patterns pose a challenge to the management of water resources systems as these systems are designed to maintain a fragile balance between water supply and demand. With the projected changes, this balance is likely to be disrupted, ultimately requiring adaptation of the existing infrastructure. In many water resources systems *reservoirs* are the key element to ensure a stable water supply. Adaptation is difficult however, as reservoirs can be characterized as rather inflexible types of infrastructure. Increasing storage capacity is in most cases not feasible and relocation is impossible after construction. It can be concluded that alternative adaptation strategies are required to prevent performance losses associated with changing patterns of water supply and demand.

For reservoirs one of the few feasible options is to adjust their operation (Schumann, 1995). This so called dam reoperation is however a complicated procedure, since reservoirs are not only used to fulfill water demand. Several other, often conflicting, purposes are common, such as generation of hydroelectric power, downstream discharge regulation, recreation and fishery. Another complicating factor to reoperation is the fact that reservoirs are seldomly operated as a single unit. Rather are they organized as so called *multireservoir systems*: multiple cascaded or parallel reservoirs along a single river. As upstream reservoirs largely determine the inflow into downstream reservoirs, an integrated assessment of the operation of such systems is necessary.

1.2 The dam reoperation challenge

As the construction rate of new reservoirs has steeply decreased in recent years, there is currently a lot of attention from the scientific community to optimize the operation of existing reservoir systems (Labadie, 2004). Optimization of reservoirs (and in particular multireservoir systems) is a complicated process with high computational requirements. Computer hardware and software limitations in the past have required simplifications and approximations to optimization models that operators were unwilling to accept. Simulation models have therefore been applied for decades to derive decent operating rules by trial-and-error (Wurbs, 2003).

However, recent developments have led to a new generation of computationally efficient techniques that are able to optimize multireservoir systems in an integrated way. These *Metaheuristic Algorithms* (MA) have been applied successfully to reservoir systems with various configurations, often resulting in better operating rules than the ones currently being used (Oliveira and Loucks, 1997; Chen et al., 2007; Kumar and Reddy, 2007; Chang and Chang, 2009; Fu et al., 2011; Liu et al., 2011; Ostadrahimi et al., 2012).

Despite these new opportunities, Labadie (2004) argued that still many large reservoirs worldwide do not produce the level of benefits that once provided the economic justification for their development. The reason does not necessarily lie in shortcomings to the optimization techniques. An inadequate consideration of the operations and maintenance issues once a project is completed is a more likely reason. Throughout the years performance can also be undermined when new uses arise that were not considered in the planning phase. Frequent re-evaluation of the reservoir operating rules is therefore important to maintain and, whenever feasible, increase reservoir performance under changing circumstances during its lifetime. However it is yet unclear to which degree of water supply and demand changes dam reoperation is still possible.

Dam reoperation may be a solution to mitigate the effects of climate change as this is expected to severely influence river discharge. Several studies have recently been published on the impacts of climate change on hydrological regimes. These works generally incorporate one or more climate change projections into a hydrological model (Minville et al., 2009). However, only few studies have investigated the adaptation of water resources systems in detail. One of the rare examples is a case study of Minville et al. (2010), who analyzed the impact of climate change on water resource management of the Peribonka River System in Canada. They concluded that reservoirs can become less *reliable* and more *vulnerable* and that reservoir operating rules should be re-examined in order to take account of a changing hydrology due to climate change.

Payne et al. (2004) conducted a similar study for the Columbia River Basin, USA. They concluded that climate change is likely to have a severe impact on the performance of reservoirs in the basin. Several adaptation strategies for reservoir operation were investigated using the ColSim simulation model. However, the authors did not conduct a full-scale automated reoperation of the reservoir.

Schumann (1995) and Raje and Mujumdar (2010) are one of the few authors that actually investigated the flexibility and adjustability of reservoir operation in case of a large shift in water supply and demand patterns. In both studies a new optimization of operating rules is proposed and demonstrated as a suitable adaptation strategy. However, the adaptability of more complex cascade reservoir systems is yet uninvestigated. The question remains open whether or not it is really effective to adapt such systems to changing supply and demand patterns just by dam reoperation.

1.3 Study area

The sub-provincial city Hangzhou, located in Zhejiang Province (southeast China), was selected as study area. Hangzhou is a region covering about 16,850 km^2, governed as a so called sub-provincial city. It contains a metropolitan area as well as a surrounding rural area with smaller sattelite cities and villages (Figure 1.1). The metropolitan area is administratively divided into 8 densely populated districts, commonly referred to as the Hangzhou urban districts. The rural part of *Hangzhou Region* is divided into 5 districts: Fuyang City, Tonglu County, Lin'an City, Jiande City and Chun'an County.

The population in the region is mainly concentrated in the metropolitan area, close to the mouth of Qiantang River. The major center of industrial activity is Xiaoshan, a coastal plain south of the river. Currently more industrial zones are developed further along the Fuchun River branch. Medium to small scale enterprises are predominant in the river basin, of which the light industries mainly produce paper, food, textile and arts and crafts. The heavy *industrial output* covers machinery, chemicals, metal components and construction materials. Water consumption of these industries is high.

A large part of Hangzhou Region is located in the Qiantang River Basin. This basin is situated between east longitudes 118° to 121° and north latitudes 28° to 31° and covers a total area of 55,558 km^2. Qiantang River has several large tributaries. It meanders through mountainous terrain, urban areas and coastal plains from southwest to northeast, ultimately draining in the East China Sea (see Appendix A).

The largest upstream branches, Xin'an River and Lan River, originate in mountainous areas and confluence in the center of the catchment. From this confluence point the river continues as the Fuchun River. Smaller tributaries, Fenshui River and Puyang River, flow into this main branch. At the confluence point with the latter, just before entering Hangzhou City, the name becomes Qiantang River. At the mouth of the river, in Hangzhou Bay, the average discharge is 1043 m^3s^{-1}. The discharge regime is characterized by a high flow period between March and July and a low flow in the remaining months.

Nearly the entire Hangzhou Region relies on surface water from the Qiantang River for its supply. Water is abstracted directly from the river through various intakes. The only exception is the district Lin'an City, where groundwater is used. No serious water shortages have occurred in recent years, yet water quality remains an important issue. Pollution from upstream river sections and salt water intrusion at the river mouth pose a risk for the various downstream water intakes of water purification plants.

Two cascaded reservoirs are used to maintain a stable water supply: Xin'anjiang Reservoir upstream and Fuchunjiang Reservoir further downstream. Next to their important role in water supply, the reservoirs have other competing purposes such as flood control and hydropower generation. Operation of the reservoir cascade has recently gained attention from local policy makers as its releases are crucial for preventing downstream salt water intrusion.

Hangzhou Region is particularly suitable for our study as it currently faces rapid population growth and economic development. These developments are, in combination with climate change effects, expected to cause an increasing stress on the water availability. All data relevant for this study have been monitored for an extensive period and are available in statistical records and hydrological datasets. Currently the reservoirs in the area are operated independent of each other. Coordinated dam reoperation could therefore be a potential solution to relieve the area from its projected future water stress.

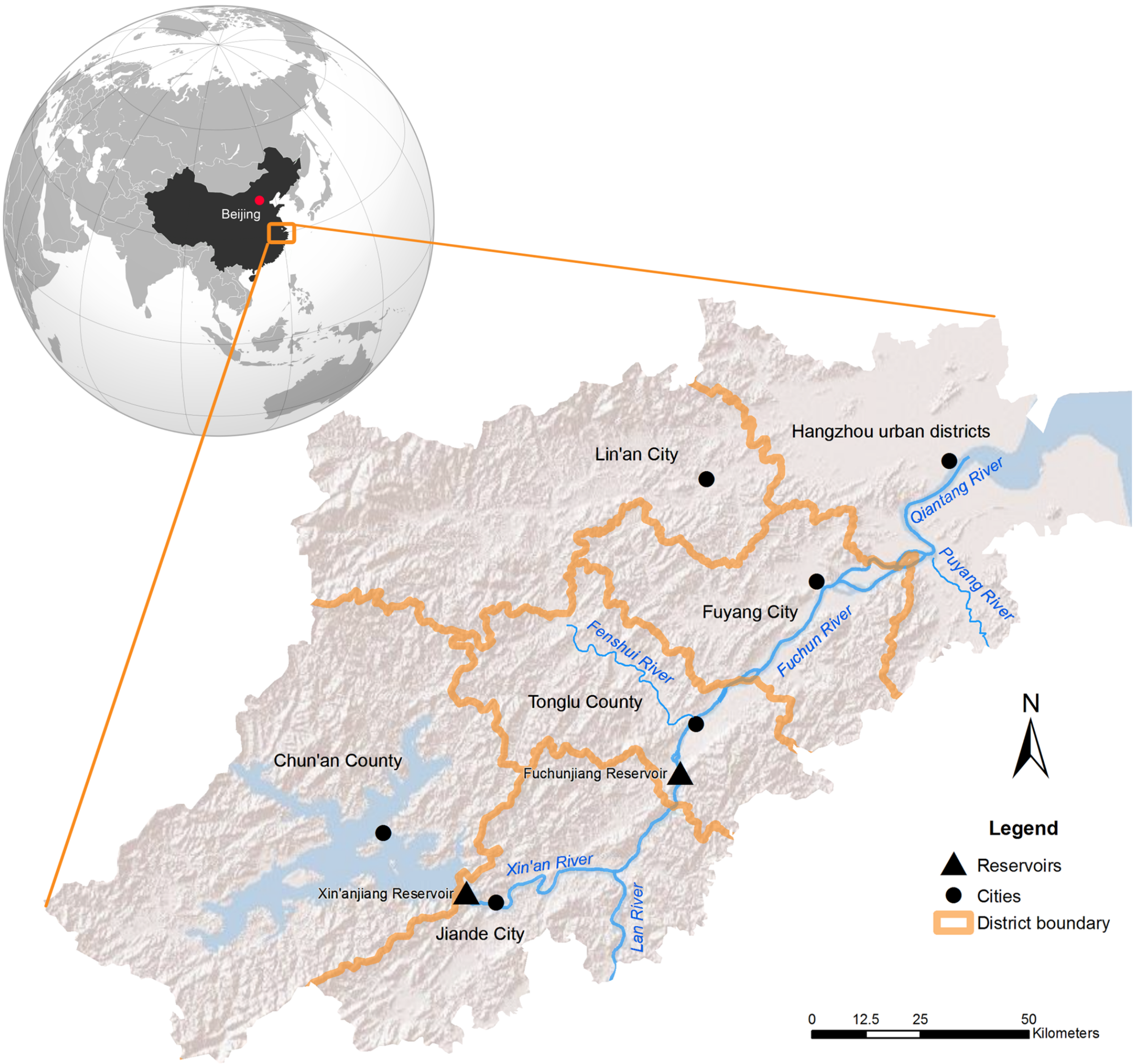

Figure 1.1: Administrative division of Hangzhou Region and location of the relevant elements of the water resources system.

1.4 Research objective and questions

The objective of this research project is defined as:

To investigate whether reoperation of the Xin'anjiang-Fuchunjiang reservoir cascade is an effective adaptation strategy to mitigate potential impacts of climate change and regional socio-economic developments.

In the context of this objective we define the effectiveness of an adaptation strategy as its ability to restore the performance of a system to its original situation. The following five questions are used as a guideline towards the objective:

1. What are the relevant aspects regarding current operation of the reservoir cascade?
2. What is the likely extent to which climate change and socio-economic developments could impact the future patterns of water supply and demand?
3. How can the relevant aspects of the water resources system be included in a model for simulation and optimization of cascade reservoir performance?
4. What is the impact of the projected changes in water supply and demand on the performance of the reservoir cascade under current operating conditions?
5. How much performance can be gained by coordinated reoperation of both cascade reservoirs?

1.5 Research approach and thesis outline

The research questions logically ensue from the underlying research model (Figure 1.2). Each chapter of this thesis covers one research question. In Chapter 2 the design features and operation of both cascade reservoirs are discussed (research question 1). The methodology (questions 2 and 3) is addressed in Chapters 3 and 4.

Chapter 3 describes the method for reconstruction of historical water demands and the forecasting of future water supply and demand. We consider the impact of climate change and socio-economic developments during the future period 2011-2040 and compare this to the control period 1971-2000. As we want to investigate the reoperation potential of the reservoir system, we follow a scenario-based approach to explore the effects of various degrees of likely supply and demand changes. To this extent we consider three underlying socio-economic forces on the demand side (population growth, industrial production and changing land use) and climate change as underlying process influencing the supply side. For each process three equally likely future development trajectories are identified. The resulting water stress scenarios are based on four extreme combinations of these processes and a middle scenario (Figure 1.3).

The tool that plays a central role in the methodology of this research project is a water allocation model interlinked with an optimization algorithm. Water supply and demand data are the actual input for this model, for which the setup is described in Chapter 4. This chapter also introduces the optimization module used to derive adapted reservoir operating rules. In this study only the long-term operating rules are subject to optimization. Possible physical changes of the dams and other infrastructure in the future are outside the scope of this study.

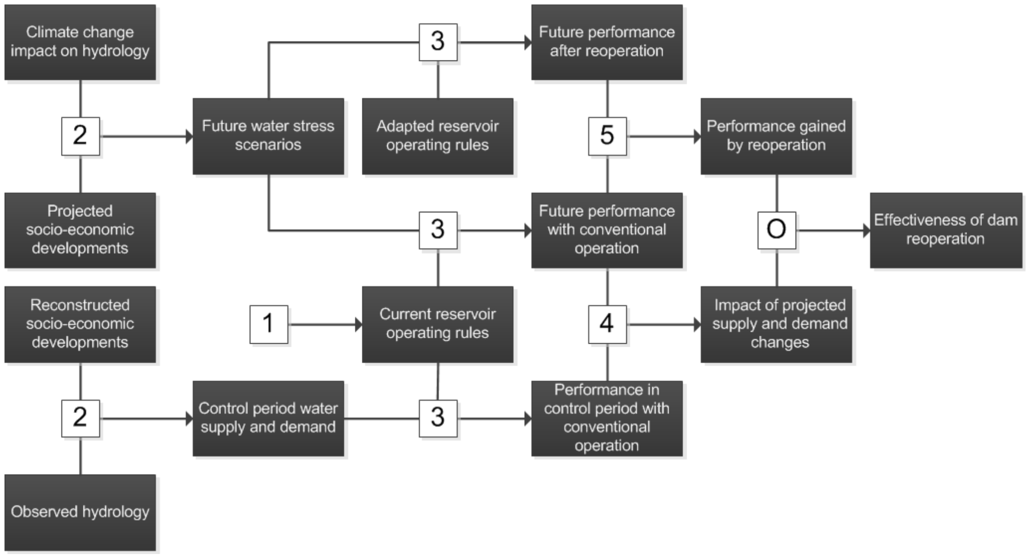

Figure 1.2: The underlying structure behind this thesis. The numbers correspond to the research questions, which follow the same sequence as the chapters in this thesis. The answer to each research question is found by combining and comparing the related research objects, thereby reasoning towards the final conclusion on the right side of the scheme. The objective (O) is achieved by comparing the performance of conventional operating rules with adapted operating rules in the future period.

The water allocation model is used to evaluate the current reservoir performance and possible future performance. This reservoir performance is defined as the net social and economic benefit generated by the reservoir system, expressed in terms of water shortages and hydropower production. Performance of the reservoir system with the conventional operating rules is presented and discussed in Chapter 5. These results are then compared with the reservoir performance after reoperation in Chapter 6. Finally, Chapter 7 combines all the individual research questions and gives the conclusions and recommendations.

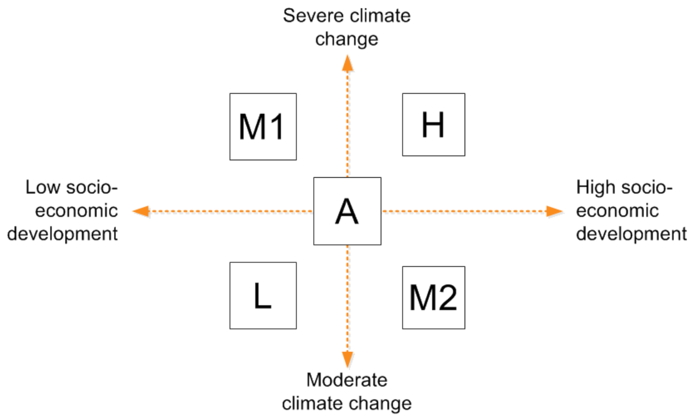

Figure 1.3: The five water stress scenarios considered: Low (L), Moderate 1 (M1), Average (A), Moderate 2 (M2) and High (H).

Chapter 2

The Xin'anjiang-Fuchunjiang reservoir cascade

In this chapter the relevant aspects regarding the current operation of the Xin'anjiang-Fuchunjiang reservoir cascade are discussed, thereby answering the first research question. Section 2.1 introduces the location and purposes of the reservoir cascade. Detailed operation of Xin'anjiang Reservoir and Fuchunjiang Reservoir is addressed separately in Section 2.2 and 2.3, respectively.

2.1 Overview

The outflow from Xin'an subbasin is nowadays completely controlled by Xin'anjiang Reservoir (Figure 2.2), also known as the Thousand Islands Lake. It is by far the largest *reservoir* in the Qiantang River Basin. The dam was constructed between 1957 and 1960 and it has been in continuous operation ever since. Its design can be described as a concrete gravity dam with ogee crest and controllable *spillways*. About 67 km downstream of Xin'anjiang Reservoir, a smaller dam has been build: Fuchunjiang Reservoir. It was completed in 1968. The river-style reservoir has a long and narrow shape, with a length of about 26.5 km and a small width-length ratio.

Xin'anjiang Reservoir is operated for multiple purposes. Flood control has the highest priority, followed by hydropower production and water supply. As the reservoir itself is also used extensively for fishery and recreation, a fairly constant *pool level* is maintained with 108 m above Mean Sea Level (MSL) as target storage level. The primary functions of Fuchunjiang Reservoir are similar to Xin'anjiang Reservoir: hydropower production and water supply. Due to its relatively small size, the flood control capabilities are limited.

State Grid Corporation of China (SGCC) operates both reservoirs and supplies the generated energy to the East China Power Grid. Under normal circumstances the operations of Xin'anjiang Reservoir are independent to those of Fuchunjiang Reservoir. Only during potential flood events the operators switch to an emergency control system that coordinates the spillway releases of both reservoirs. Sedimentation is currently not a significant issue, such that sediment *flushing* or *sluicing* is not considered in the release rules.

Table 2.1: Design characteristics of Xin'anjiang and Fuchunjiang Reservoir (Hydropower and Water Resources Planning & Design General Institute, 2006; Zhejiang Design Institute of Water Conservancy & Hydroelectric Power, 2006). A more detailed description is given in Appendix C.

Category	**Aspect**	**Xin'anjiang Reservoir**	**Fuchunjiang Reservoir**	**Unit**
Dam and reservoir layout	Reservoir capacity ratio[1]	1.33	0.03	-
	Total storage capacity	21.63	0.885	10^9 m^3
	Dead storage	7.57	0.076	10^9 m^3
	Dam crest level	115	32.2	m+MSL
	Maximum water level	114	28.2	m+MSL
	Normal tailwater level	22.6	7	m+MSL
	Minimum pool level	86	11.6	m+MSL
Spillways	Spillway crest level	99	11.6	m+MSL
	Spillway capacity	14000	32640	m^3s^{-1}
Hydropower works	Installed capacity	810	360	MW
	Number of penstocks	9	6	-
	Total penstock capacity	1291.5	3000	m^3s^{-1}
	Penstock intake level	70.4	15	m+MSL
	Firm power output	160	128	MW

2.2 Xin'anjiang Reservoir operations

To deal effectively with the uncertain water demands and inflows, Xin'anjiang Reservoir uses two complementary operation modes for different time scales. Long-term operating rules prescribe reservoir releases throughout a hydrological year with 10-day time increments. Short-term operation is embedded within this framework, tracking the long-term guidelines over shorter time horizons in hourly time increments. Short-term releases are guided with decision support systems that use energy demand, upstream discharge measurements, reservoir storage levels and meteorological forecasts as input.

The long-term release decisions are based on the so called reservoir zoning. Currently the reservoir has a total of five storage zones. The elevation of each zone varies throughout the year and is guided by a corresponding *rule curve* (Figure 2.1). Every storage zone has its own set of rules (zone rules) that prescribe the quantity of water to be released. Whenever the water level is in a certain zone, the corresponding release rules of that zone apply (Table 2.2). Typically, one zone rule specifies the downstream supply requirement and a second zone rule the hydropower production target.

For the *flood control zone* (I), spillway gates will be opened and operators are required to release water at full discharge capacity Q_{max}. For zones II to IV the total releases R in each operational period j are equal to the downstream supply requirement F or the hydropower production requirement, whichever is highest. The lowest storage zone (V) uses *hedging* rules, which guide the rationing of water whenever shortages are likely to occur. For this zone the actual releases are restricted 70% of the inflow I. This is used to limit the impact of water shortage in a later stage of the drought and smoothen deficit fluctuations (Srinivasan & Philipose, 1998).

[1] The capacity ratio is defined as the active storage capacity of the reservoir relative to the mean annual inflow.

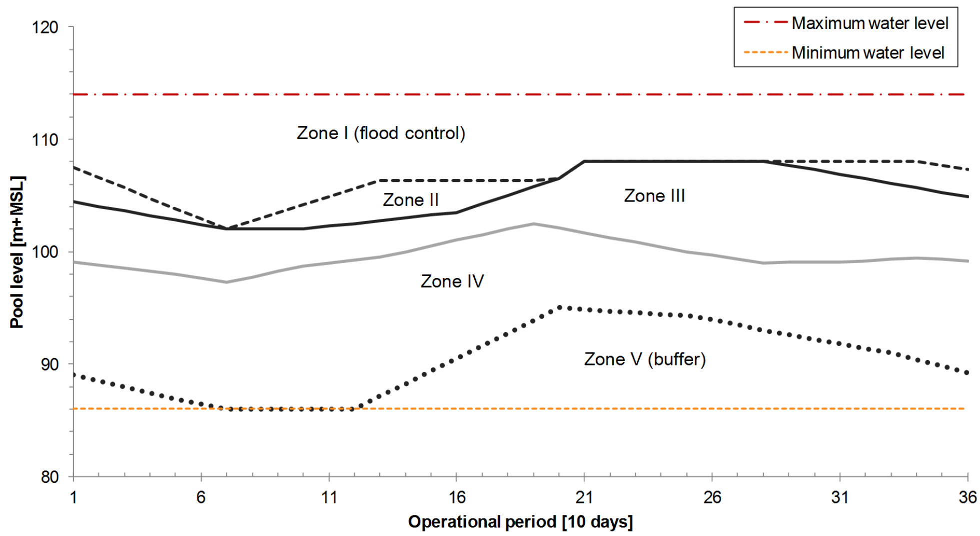

Figure 2.1: Reservoir zoning and rule curves of Xin'anjiang Reservoir. The first operational period corresponds with the start of the calendar year.

Hydropower production targets for each operational period are set by the operators based on inflow forecasts, current reservoir storage levels, interannual inflow patterns and personal experience of the operators. In this study linear hydropower production rules are adopted for each storage zone to reflect the human decision making process, thereby incorporating all aforementioned factors. Table 2.2 shows that the energy production E is based on the reservoir active storage at the beginning of the current operational period $S_{a,j}$ and total forecasted inflow volume during the current operational period I_j.

A clear seasonal pattern is observed in the historical release decisions for zones III and IV. We therefore define seasonally varying coefficients for the hydropower production rules of these zones. The coefficients for zone II are assumed not to vary seasonally as the reservoir storage only occasionally reaches such high levels. Coefficients of the production rules are determined by model calibration (Section 4.4).

Within the long-term framework the hydroelectric station is operated as a *load-following plant*. The plant is normally dispatched during daytime and early evening, which are the periods when the electricity demand is the highest. As a result of these operating rules, the electricity output is highly intermittent. Yet on a long-term basis, the operators must guarantee a minimum average output of 160 MW. All energy that is produced in addition to this so called *firm power* output is defined as *secondary energy*.

Table 2.2: Zone rules for Xin'anjiang Reservoir.

Zone	**Water supply rule**	**Hydropower production rule**
I	$R_j = Q_{max}$	-
II	$R_j = F_j$	$E_j = a_2 + b_2(S_{a,j} + I_j)$
III	$R_j = F_j$	$E_j = a_{3,s} + b_{3,s}(S_{a,j} + I_j)$
IV	$R_j = F_j$	$E_j = a_{4,s} + b_{4,s}(S_{a,j} + I_j)$
V	$R_j = 0.7 I_j$	-

Power plant usage can be expressed as a so called *plant load factor*, which is often defined as the ratio between average power load on the plant for a certain period divided by the *installed capacity*. For Xin'anjiang Reservoir this factor is 21.5%. It is related to out-of-service periods reserved for maintenance, fluctuations in electricity demand and projected water availability.

2.3 Fuchunjiang Reservoir operations

Fuchunjiang Reservoir is currently operated as a *base load plant*, delivering so called *Run-Of-River (ROR) hydroelectricity*. The electricity output is highly variable, as in each 10-day operational period the reservoir approximately releases the same volume as the forecasted inflow. This inflow in turn is determined by the releases from Xin'anjiang Reservoir and the discharge from the Lan River branch. On average the *spillways* are opened for approximately 30 days per year to enable passage of high water waves.

The spillway crest level of Fuchunjiang Reservoir is governing for the size of the *dead storage* zone. On top of this zone is a *conservation pool* with a fixed elevation between 11.6 m+MSL (spillway crest) and 24.7 m+MSL. The *flood control zone* also has a fixed elevation, with its top (maximum water level) at 28.2 m+MSL. With the current operation style, streamflow is regulated on a daily timescale. Annual flow regulation is not possible due to the low capacity ratio (Table 2.1). Yet for the dry season, when the inflows are generally low, flow regulation on a seasonal timescale could be feasible. This could possibly reduce the total amount of spills, with beneficial effects such as a higher electricity production and less water shortages.

Figure 2.2: Xin'anjiang Reservoir (top) and Fuchunjiang Reservoir (below).

Chapter 3

Supply and demand dynamics

This chapter explains the first part of the methodology: computation of historical water supply and demand and estimation of their future development. As guided by the second research question, we identify the likely extent to which climate change and socio-economic developments could impact the future patterns of water supply and demand. From the demand-side perspective we assess the socio-economic trends in order to reconstruct the historical water demands as well as to make projections of the future water demand. The demand-side processes are investigated in Section 3.1. Climate change, as predominant process on the supply side, is discussed in Section 3.2. The resulting annual water supply and demand patterns are presented in Section 3.3.

3.1 Demand side processes

Water demand is considered for each district separately to account for spatial variability. Within each district, different demand categories are considered: *domestic* and *municipal demand*, *industrial demand* and *agricultural demand*. We use linear demand functions to estimate the annual water demand, thereby considering a distinct underlying driving force for each demand category (Figure 3.1). For example, the domestic water demand is obtained by multiplying the population size with the water demand per capita (thereby further distinguishing between urban and rural population). It is assumed that the unit demand rate does not change significantly throughout time.

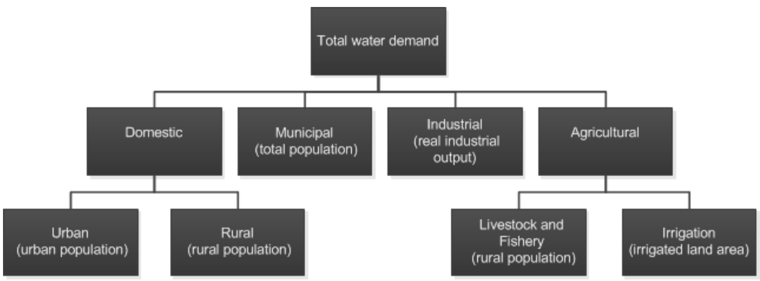

Figure 3.1: Hierarchy of the water demand categories and the respective driver for each category. Driving forces are localized to district-level.

Socio-economic data per district were obtained for recent years (2007-2010) from the Hangzhou Bureau of Forestry & Water Conservancy (2008). Since this localized data were not available for the entire control period, regional-average growth rates have been used to reconstruct the historical urban and rural population, *industrial output* and irrigated land area per district. The aggregated growth rates for *Hangzhou Region* were retrieved from the China Economic and Social Statistics Database (CNKI, 2013). For the year 2000, reconstructed socio-economic data are shown in Table 3.1. The Lin'an district is excluded in this analysis since it relies on groundwater abstractions for its water supply.

Localized unit demand rates have been calculated based on the actual water demand per district in recent years (Hangzhou Bureau of Forestry & Water Conservancy, 2008). A complete overview of the used methodology and the resulting unit rates is given in Appendix B. The specific methodology for each separate socio-economic process is discussed in the following subsections.

As only annually aggregated water demand could be obtained from literature, the seasonal variations herein have been estimated. The CROPWAT method (FAO, 2012a) was used for seasonal variation of irrigation water demand, and the variations in *domestic demand* were estimated as a function of temperature (Wada et al., 2011). *Industrial demand* and demand for livestock and fishery is assumed to be constant throughout the year. The details of seasonal demand estimation are presented in Appendix B.

Table 3.1: Population and irrigated farmland per district for the year 2000. Since the real industrial output per district could not be retrieved, the aggregate production for Hangzhou Region is used in this study. Statistics for Lin'an are excluded as it is not relevant for the water demand.

Driver	**District**					**Total**
	Hangzhou (urban)	**Fuyang**	**Tonglu**	**Jiande**	**Chun'an**	**(ex. Lin'an)**
Urban population [10^3]	1839.56	90.05	75.62	91.37	52.39	2148.99
Rural population [10^3]	1771.24	567.76	323.39	426.10	421.78	3510.27
Irrigated farmland [km^2]	979	202	145	183	62	1571
Real industrial production [10^9 RMB]	-	-	-	-	-	70.9

3.1.1 Domestic and municipal demand

The primary driver of *domestic* and *municipal* water demand is population size. Water consumption per capita appears to be significantly higher in urban areas relative to rural areas (Appendix B). To reflect this accurately in the model results, rural and urban population is considered separately. As of 2000, the total population in Hangzhou Region (including Lin'an District) was 6.2 million, of which 2.3 million people were living in urban areas and 3.9 million in the rural areas. The population is expected to grow further in the upcoming years. A clear correlation can be observed between the increase in urban population and a simultaneous decline in rural population. This urbanization trend is observed throughout China.

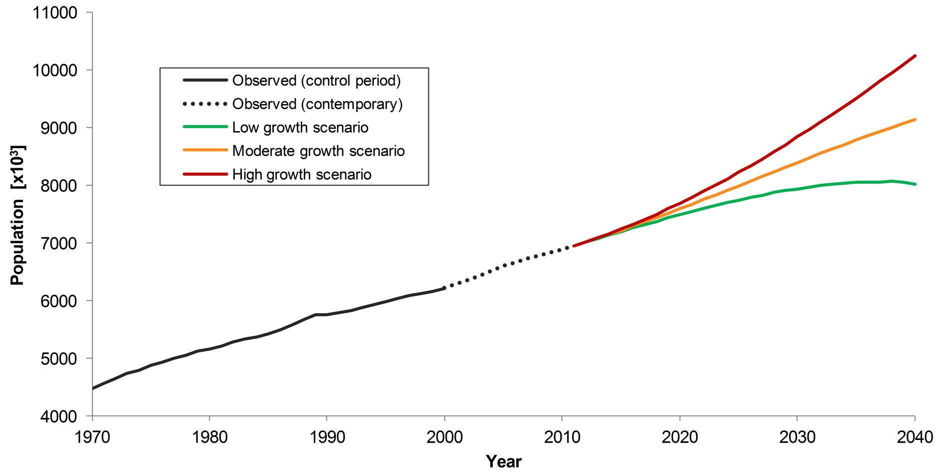

Figure 3.2: Development of the population in Hangzhou Region. Historical data were obtained from the China Economic and Social Statistics Database (CNKI, 2013). The 2040 projections for the low, middle and high growth scenario are around 8, 9 and 10 million, respectively.

Based on trends in the historical population dynamics and projections (Zhejiang Design Institute of Water Conservancy & Hydroelectric Power and Zhejiang Institute of Hydraulics & Estuary, 2005), three scenarios were constructed for the future. For the high growth scenario we assume a steady annual growth in the urban districts of 3%, while the population decline of the rural areas changes steadily from -1.5% to 0%. The low growth scenario assumes a change in growth in urban districts from 3% in 2010 to 0.5% in 2040. The population decline in the rural areas is assumed to stabilize slowly from the current -1.5% to about -2% in 2040. For the moderate growth scenario a decline of the rural population up to -1% per year in 2040 is projected in combination with a linearly decreasing growth of the urban population of 3% in 2011 to 1.3% in 2040.

3.1.2 Industrial demand

Water required for industrial processes is assumed to be proportional to the total production of the secondary sector of the economy. Therefore we use the real *industrial output* as measure for the industrial demand (Loucks and Van Beek, 2005). The nominal industrial output for Hangzhou Region was obtained from the China Economic and Social Statistics Database. These data were corrected for inflation using the GDP implicit deflator records for China (The World Bank, 2013), with 2000 as index year.

Between 2000 and 2010, the average growth of the real industrial output was 10% per year. Future scenarios were developed by extrapolation of current trends and economic forecasts according to Wang et al. (2007) and Wang et al. (2010). For the high growth scenario a continuing expansion of the industrial output is assumed, with a linearly declining growth rate stabilizing at 5.5% in 2025. The low growth scenario assumes a similar decline towards a rate of 1.5% in 2025 (remaining constant at this rate afterwards). For the average scenario we project a gradually declining growth towards 1.5% in 2040.

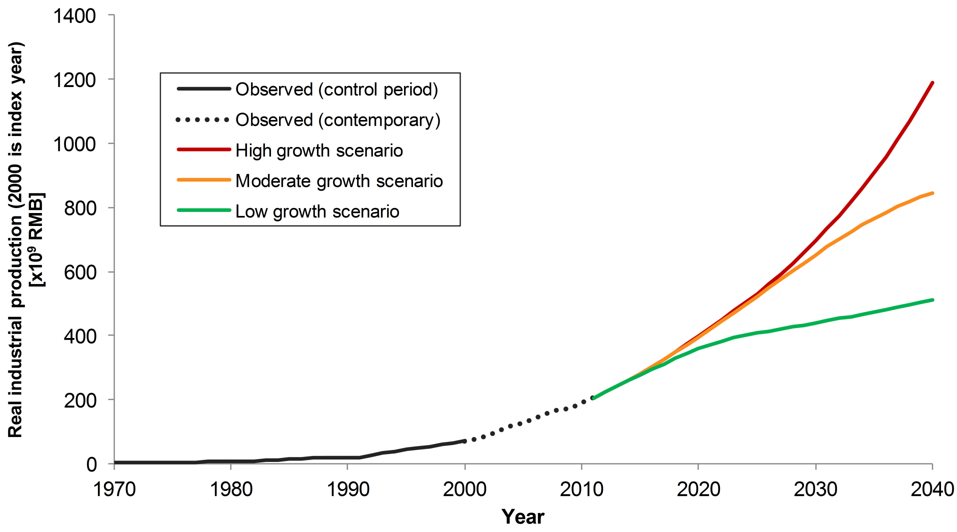

Figure 3.3: The real industrial output of Hangzhou Region. Historical nominal industrial output was obtained from the China Economic and Social Statistics Database (CNKI, 2013) and corrected for inflation. Compared to the year 2000, a nearly 17 fold increase to 1187 billion RMB is expected for the high growth scenario in 2040. The low and moderate growth scenario assume an industrial production of 511 and 845 billion RMB in 2040, respectively.

3.1.3 Agricultural demand

The largest portion of all water being withdrawn from the Qiantang River is used for agricultural purposes. This water is mostly used for irrigation, drinking water for livestock and to fill fishing ponds. As livestock is kept on a small scale by farmers in the study area, it appears to be strongly correlated to the rural population size. The total area of irrigated farmland is considered as driving force for the irrigation water demand.

The amount of irrigated land appears to fluctuate throughout the control period. From 1970 to 1985, the total area increased due to forest logging. However, after 1985 the total area declined gradually as more and more land was redeveloped to facilitate expansion of the urban areas and industry. In recent years this decline has stopped, which can be attributed to the development of new land area and the shift to new crop types. Whereas the production of rice was dominant in the past, recently so called *cash crops* have become more popular due to higher profit margins.

As of 2000, the region had about 1708 km^2 of irrigated farmland (1571 km^2 excluding Lin'an District). Most of the land is used to grow *staple crops* such as rice, wheat, corn, soybean and potato. In addition several *cash crops* such as tea, cotton, sugarcane and medicinal herbs are common. Nevertheless, rice is still the prevailing crop type as it covers about 85% of the total cultivated area.

There is no clearly observable trend in recent developments. Therefore various alternative developments are explored for the future scenarios. The moderate scenario assumes no significant change. The two extreme scenarios assume a gradually increasing decline in land surface and a constant increase respectively (Figure 3.4).

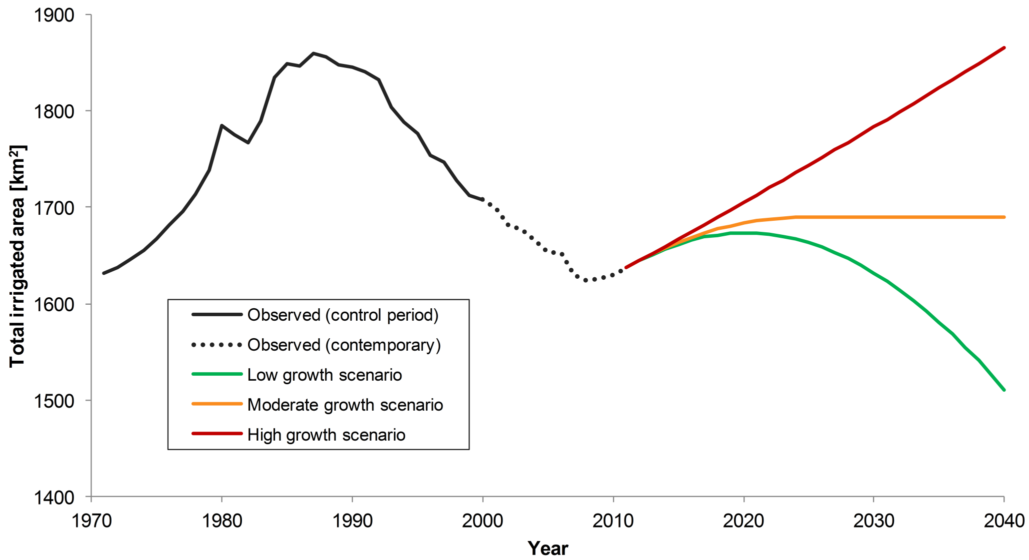

Figure 3.4: Development of the total irrigated area in Hangzhou Region. Data were obtained from CNKI (2013).

3.2 Supply side processes

Daily streamflow records of Lan River and monthly inflow records for Xin'anjiang Reservoir were obtained for the entire control period. Those were preprocessed to 10-day averaged timesteps (Appendix A). For the future period the hydrological regime is expected to change due to the effects of climate change. Additional climate change effects on the demand side, such as a potentially increasing irrigation water demand, are outside the scope of this study since aggregated uncertainty herein is already reflected by the various scenarios. The discharge of small tributaries such as Puyang River and Fenshui River are assumed equal to the control period.

Projected streamflows for the future period were obtained using the GR4J rainfall runoff model (Perrin et al., 2003). This model was calibrated separately for the Xin'an and Lan subbasins. The input for the hydrological simulations was obtained by dynamic downscaling of global climate simulations using the HadRM3P Regional Climate Model (RCM). The RCM is implemented in the PRECIS modelling system and yields output on a daily timescale with a spatial resolution of 0.5° by 0.5°. HadRM3P is driven by the HadCM3 Global Circulation Model (GCM). The A1B, A2 and B2 SRES greenhouse gas emission scenarios are evaluated in this study.

For each subbasin the daily simulated precipitation and temperature were compared to the corresponding observed values for the period 1971-2000. To this extent all observed data have been interpolated to area-average values using Thiessen polygons. The grid-based RCM output was converted by taking the weighted average of the cells overlapping the basin area. The weights have been determined as the fraction of the subbasin area falling within a grid cell.

Comparison of the averaged precipitation and temperature showed a significant bias. We applied a bias correction for each individual subbasin as there seems to be a consensus among most authors that this is a necessary step in order to match the RCM data with the observations (Leander and Buishand, 2007; Terink et al., 2009).

A simple multiplicative shift method was used to correct the bias of the subbasin-averaged daily RCM rainfall:

$$P^*_{s,d} = \frac{P_{o,m}}{P_{s,m}} P_{s,d} \tag{3.1}$$

In this equation the simulated daily precipitation amount $P_{s,d}$ is transformed to a corrected amount $P^*_{s,d}$ with the ratio between mean monthly observed precipitation $P_{o,m}$ and mean monthly RCM simulated precipitation $P_{s,m}$. This procedure adjusts only rainfall intensity to reproduce the long-term mean observed monthly rainfall, and therefore does not correct any systematic error in frequency or the intensity distribution. However, Ines and Hansen (2006) concluded that in most cases this method provides similar results compared to a more complicated frequency-intensity correction.

A similar bias correction method is used for temperature to adjust the monthly mean:

$$T^*_{s,d} = T_{s,d} + (T_{o,m} - T_{s,m}) \tag{3.2}$$

The corrected daily temperature $T^*_{s,d}$ is obtained by adding the difference between observed monthly temperature $T_{o,m}$ and RCM simulated monthly temperature $T_{s,m}$ to the simulated daily temperature $T_{s,d}$. The resulting data after bias-correction are used as forcing for the hydrological models. Hamon's equation (Hamon, 1961) is used to convert temperature to evaporation.

The impact of each climate change scenario is assessed by analyzing the simulated discharge of the GR4J model. As in this study drought periods are considered critical, the simulation results (2011-2040) are compared and ranked based on the average discharge (Table 3.2). The B2 scenario has the lowest total inflow and is therefore selected as the most severe scenario for this particular study area. The A2 scenario has the highest average discharge and is regarded as the least severe scenario. Finally, A1B is selected as middle scenario.

Table 3.2: Mean and standard deviation of the 10-day averaged discharge in each streamflow dataset.

Dataset	**Mean (st. dev.) [m^3s^{-1}]**		
	Lan River	**Xin'an River**	**Total**
1971-2000 (control period)	543 (692)	349 (352)	892 (776)
2011-2040 (A1B)	509 (840)	295 (469)	804 (962)
2011-2040 (A2)	491 (915)	315 (557)	806 (1071)
2011-2040 (B2)	482 (875)	309 (530)	791 (1023)

3.3 Water supply and demand totals

The total water supply requirement is defined as the water demand plus the annual volume required to satisfy the governing instream flow requirement. The water demand unit rates as shown in Appendix B are applied to obtain annual volumes for each category. In addition, the governing flow requirement for *Hangzhou Region* is the minimum flow required at the mouth of Qiantang River (Zhejiang Design Institute of Water Conservancy & Hydroelectric Power and Zhejiang Institute of Hydraulics & Estuary, 2005). In reality the exact minimum flow requirement has been altered several times. However, in this study we use the most recent formulation of this requirement and assume that it is constant for both the control period and future period.

The minimum discharge should be guaranteed at all times in order to limit pollution concentrations, control sedimentation, enable navigation and prevent downstream salt intrusion. During the high-water period from April to June an average flow of about 700 m^3 s^{-1} is required. During the dry season the prescribed minimum flow is reduced to about 200 m^3 s^{-1}. The annual volume required is approximately 10.3 billion m^3.

From Figure 3.5 it can be observed that there was abundant water available throughout the control period, which is in line with observations and previous studies (Daixin et al., 2005). Yet, for all future scenarios there are periods in which the water supply requirements exceeds the inflow. Despite the regulation ability of the reservoirs in the area, these results suggest that water stress is likely to occur in the future. The significant increase in water demand seems to be a major disrupting factor in the water balance.

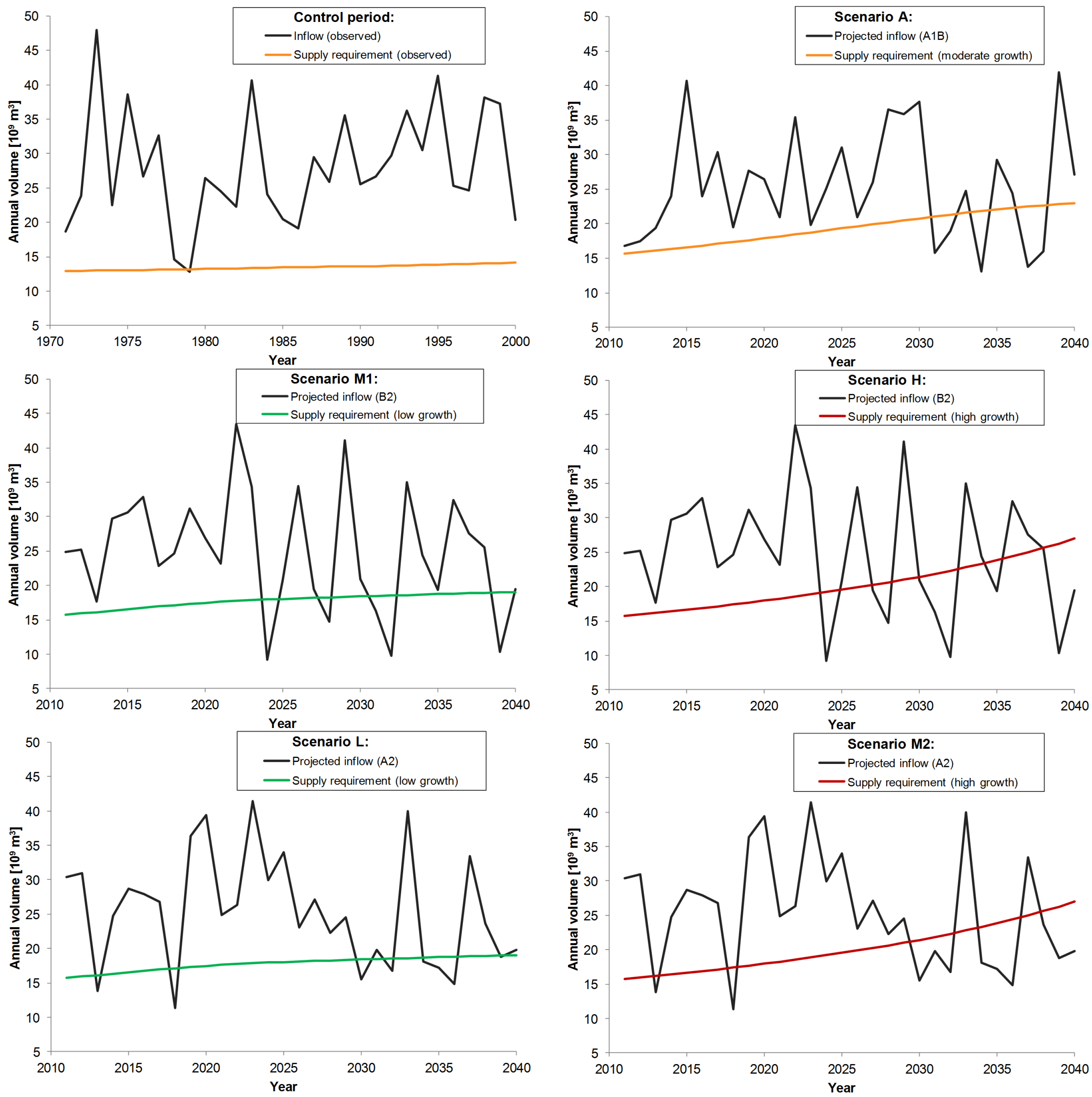

Figure 3.5: Annual inflow and supply requirement (water demand and flow requirements) for the control period and the five scenarios.

Chapter 4

Model setup

Based on the third research question, we investigate in this chapter how the relevant aspects of the water resources system can be included in a model for simulation and optimization of cascade reservoir performance. The overall modelling framework is presented in Section 4.1, after which the setup of the simulation module (Section 4.2) and the optimization module (Section 4.3) is explained in more detail. The optimization module is employed twice: first for calibration of the water allocation model (discussed in Section 4.4) and in a later stage for optimization of the reservoir operating rules (Section 4.5).

4.1 Modelling framework

Performance of the reservoir system is computed as a function of hydrologic fluxes within the river basin, water demands and reservoir operating rules. The complexity of such calculations requires a water allocation model that simulates the distribution of water volumes on a river basin scale. Such models generally do not include hydrodynamics, but only compute volumes and fluxes throughout a chosen simulation period.

For the computation of optimal operating rules, the water allocation model is coupled to an external optimization algorithm. A direct Parameterization-Simulation-Optimization (PSO) approach is chosen for this interlink. In this approach the reservoir *rule curves* are optimized directly using a *Metaheuristic Algorithm* (MA). Compared to traditional optimization methods, such as Linear Programming, Nonlinear Programming and Dynamic Programming, MAs offer great computational efficiency. Furthermore, there are no limits to the objective function and constraints in terms of nonlinearities, non-convexity, discontinuities and the amount of decision variables (Rani and Moreira, 2010).

As illustrated in Figure 4.1, an optimization run is initiated by the MA, which generates an initial, random, set of candidate operating rules. These candidate operating rules are then subsequently fed into the water allocation model. This model simulates the behaviour and performance of the reservoir system based on the proposed operating rules. The simulation output can be used to evaluate the fitness of the *individual* candidate rules. In the next iteration step the optimization algorithm improves the *population* of candidate rules using intelligent techniques and again feeds it into the water allocation model. The iterations continue until no further improvements are found.

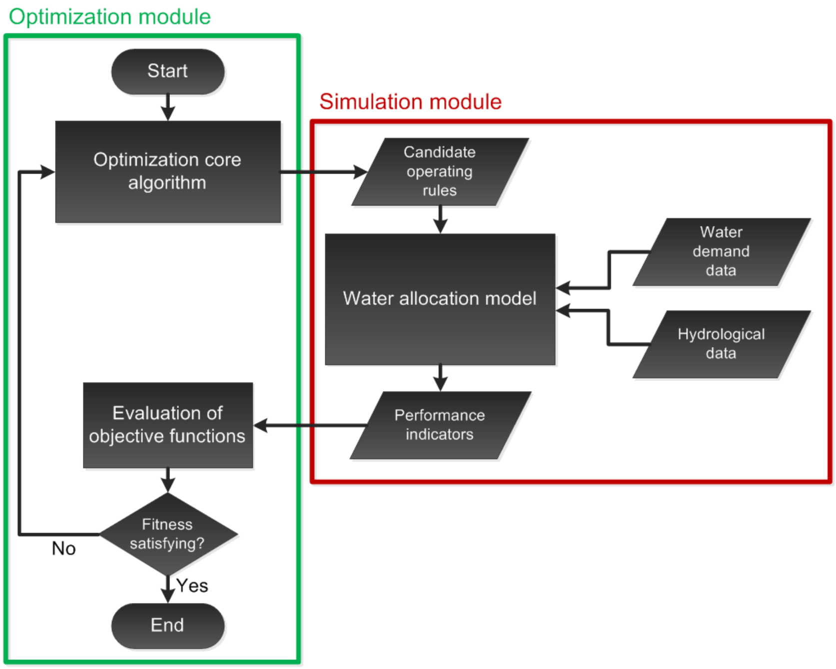

Figure 4.1: Model flowchart. The water allocation model can be used stand-alone to evaluate the performance of operating rules. For calibration and for the derivation of adapted operating rules the model is interlinked to the optimization module. NSGA-II is used as optimization core algorithm.

4.2 Simulation module

A wide variety of water allocation models have been developed in recent years. There are several software packages available, which are generally all capable of performing network systems simulation and analysis, including flood management, water supply and hydropower operations (Rani and Moreira, 2010). Most models use a network-based approach, meaning that all the features of the river basin are represented by links and nodes. Nearly all models attribute relevant information, such as inflow, physical properties, water demand and operating rules, to their respective node or link in the schematized river basin.

For this study WEAP (Water Evaluation And Planning system) has been selected as simulation tool. This model has been developed by the Stockholm Environmental Institute (SEI, 2013). Compared to other well known models, such as HEC-ResSim (US Army Corps of Engineers, 2013) and Ribasim (Deltares, 2013), it is unique in the sense that it offers great flexibility in modelling by employing an internal scripting language that can be used to define operating rules and specify custom functions and model variables. WEAP also supports interaction with external programs, which enables coupling to a separate optimization algorithm.

The study area was schematized to a system of links and nodes in WEAP. The modelling of hydropower operations is described in detail in Appendix C. To accurately model the water demands, a separate demand node was assigned to each district in *Hangzhou Region* (Figure 4.2). The total demand per district has been attributed to the different categories defined in Chapter 3: *domestic*, *municipal*, *industrial* and *agricultural demand*.

It has been considered that only a portion of the water demand is actually consumed and that the remaining part will be returned to the system after usage. Consumption rates were obtained for each individual demand category (Appendix B). The minimum flow requirement at the mouth of Qiantang River (Section 3.3) was implemented in WEAP as a time-varying constraint.

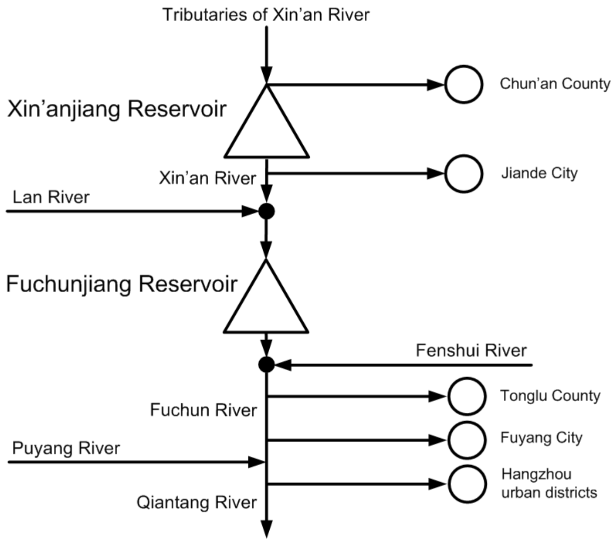

Figure 4.2: Water system diagram. The five demand districts are represented by a circle. Inflow into Xin'anjiang Reservoir is represented by a single node, while there are multiple small tributaries.

A temporal resolution of 10 days was chosen to run the simulation model. This timestep corresponds to the traditional Chinese crop calendar and is therefore the most common in reservoir operation (Chen et al., 2007; Chaves and Chang, 2008). Every month of the year is divided into three timesteps, of which the first two are exactly 10 days and the last timestep accounts for the remaining days in the month. All input data with a higher resolution are aggregated to corresponding time intervals before loaded into the model (thereby accounting for leap years).

4.3 Optimization module

4.3.1 Metaheuristic Algorithms

The core component of the optimization module is a *Metaheuristic Algorithm* (MA) that generates and improves candidate solutions and feeds these to the water allocation model. MAs are particularly suitable for solving multiobjective problems since they evaluate a large set of possible solutions during each iteration step. This way of processing yields a set of Pareto-optimal solutions within a single run of the algorithm, while traditional optimization methods require a series of separate runs (Rani and Moreira, 2010). Several MAs have been tailored specifically to multiobjective optimization. Such algorithms include additional features, such as elitism and sorting, to obtain an equal spread of solutions along the *Pareto front* (the '*solution diversity*').

```
Build random Initial Population P^0 (size N);
Set empty archive P_A^0 (size N);
Set t = 0
while t < t_max do
    evaluate Fitness Values of P^t;
    P^t = P^t + P_A^t (size 2N);
    compute Front Ranks based on Pareto dominance - sort;
    add solutions to P_A^{t+1} until N individuals have been found;
    determine crowding distance between points on each front;
    select elitist points from the lower front;
    generate Child Population P^{t+1} (size N);
      Binary Tournament Selection;
      Crossover and Mutation;
    t = t + 1;
end
```

Figure 4.3: Pseudocode NSGA-II

Most MAs are based on physical or evolutionary phenomena, the latter including Particle Swarm Optimization (PSO), Ant Colony Optimization (ACO) and Genetic Algorithms (GA). GA are most commonly used. They use crossovers and mutations to improve their candidate solutions. In the terminology of genetic programming, candidate solutions are referred to as *individuals*, who together form a *population* that evolves through time. Each individual in a population is the representation of a unique *chromosome*, which is a row vector containing all decision variables. After each iteration step, a new *generation* of individuals is formed, of which the superior ones evolve along the Pareto front.

4.3.2 NSGA-II

For this study the Nondominated Sorting Genetic Algorithm II (NSGA-II) was selected, as it is known to be highly efficient and has successfully been applied in various cases (Chang and Chang, 2009; Liu et al., 2011). The algorithm, proposed by Deb et al. (2002), can explicitly handle multiple objectives. As the subject of our optimization is a multipurpose reservoir cascade, this ability makes it favorable over many other MAs. The pseudocode is presented in Figure 4.3.

The algorithm uses features such as an elitist archive, crowding distance calculation and nondominated sorting to obtain a well-spread *Pareto front*. The first feature, elitism, is a procedure in which the fittest individuals of the previous generation are directly injected in the next generation (Luke, 2012). During each iteration step, all individuals of a generation are ranked in terms of fitness with the nondominated sorting technique. Individual A is said to Pareto dominate individual B if A is at least as good as B in every objective and better than B in at least one objective. Based on this definition, all individuals can be ranked and organized in several fronts. The front ranking and domination concepts are shown in Figure 4.4.

The so called crowding distance is used to define the density of individuals along the same front. It is calculated by the Euclidean distance between the individual and its adjacent individuals (Chang and Chang, 2009). When comparing two solutions that have the same front rank, extreme solutions prevail over not extreme ones. If both solutions are not extreme, the one with the bigger crowding distance wins (Salazar et al., 2006). In this way, a well-spread Pareto front is obtained.

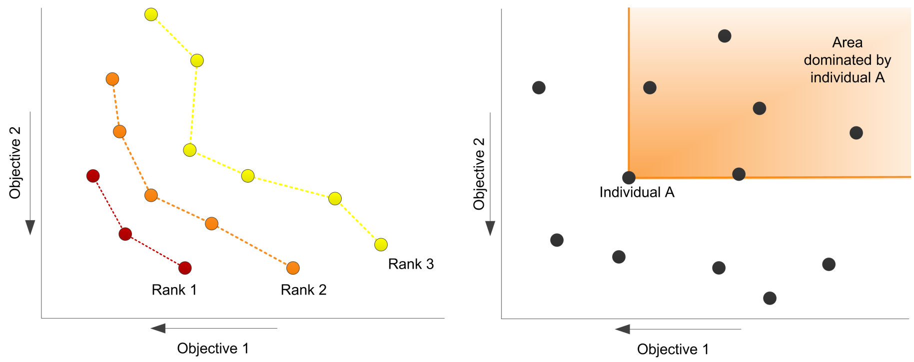

Figure 4.4: Front ranking concept (left) and domination principle (right). Each point represents an individual candidate solution.

4.3.3 Parameter settings

Chromosomes in genetic algorithms can either be binary or real coded. In this study a real-coded scheme was chosen as various authors have recently shown that this consistently yields a better performance (Kumar and Naresh, 2007; Chang et al., 2005). Each decision is subjected to two constraints: an upper and lower boundary value. A simple constraint handling technique was used, in which the algorithm repairs infeasible solutions by replacing its value by the value of the constraint that was being violated.

The main settings of the genetic algorithm were chosen based on the findings of Li and Wei (2008). Their sensitivity analysis showed that for *multireservoir systems* an optimal convergence and highest quality of the final solution is achieved with mutation and crossover probabilities of 0.05 and 0.85, respectively. The NSGA-II algorithm uses binary tournament selection, gaussian *mutation* and intermediate *crossover*. A population size of 100 individuals was chosen, as this leads to a well spread *Pareto front* and decreases the likelihood of premature convergence of the algorithm (Chang and Chang, 2001). During several test runs it was observed that no significant improvement occurs after 75 generations. Therefore the algorithm was set to be terminated after 100 generations.

4.4 Model calibration and validation

4.4.1 Method

Data available for calibration and validation of the WEAP model includes records with 10-day historical pool levels of Xin'anjiang Reservoir, 10-day releases of Fuchunjiang Reservoir and monthly hydropower production of both reservoirs. Only few aspects remained to be calibrated as most of the crucial model parameters were obtained from design reports and interviews with the operators. The calibration target parameters are:

1. Hydropower production efficiency of both Xin'anjiang Reservoir and Fuchunjiang Reservoir (2 parameters, estimated range: 70%-95%).

2. *Plant factor* (see Appendix C.2.2) of both Xin'anjiang Reservoir and Fuchunjiang Reservoir (2 parameters, estimated range: 90%-100%).

3. Coefficients of linear hydropower production rules of Xin'anjiang Reservoir for each zone (18 parameters, see Section 2.2).

The NSGA-II algorithm was employed for automatic calibration. To this extent the 22 target parameters have been encoded in a chromosome, with their likely range as optimization constraints. The Nash-Sutcliffe Model Efficiency (NSE) was used to evaluate the model predictive power for the following aspects:

1. Storage volumes of Xin'anjiang Reservoir (10-day timescale).
2. Discharge downstream of Fuchunjiang Reservoir (10-day timescale).
3. Joint hydropower production of Fuchunjiang Reservoir and Xin'anjiang Reservoir (monthly timescale).

The NSE in its general form is defined as:

$$NSE = 1 - \frac{\sum (y_{i,o} - y_{i,s})^2}{\sum (y_{i,o} - \bar{y_o})^2} \tag{4.1}$$

In this equation $y_{i,o}$ and $y_{i,s}$ respectively are the observed and simulated values at timestep i, with $\bar{y_o}$ as the mean of all observed values. The NSE ranges from $-\infty$ to 1, in which 1 indicates a perfect model fit.

A split sample test was done with 1981-1990 as calibration period and 1991-2000 as validation period. The years prior to 1981 were left out on purpose, as in that time Xin'anjiang Reservoir was operated with a set of temporary operating rules. After completion of the dam in 1960, the massive migration of inhabitants living in the area to be impounded was not yet finished. Therefore the pool levels were kept artificially low for two decades. Whereas the designed maximum water level was about 115 m+MSL, the maximum water level in this period was 102 meters. After 1981, the dam operators switched to the currently used operating rules (Zhejiang Design Institute of Water Conservancy & Hydroelectric Power, 2006).

4.4.2 Results

After calibration an overall hydropower production efficiency of 82.4% was obtained for Xin'anjiang Reservoir and 75.0% for Fuchunjiang Reservoir, with respective *plant factors* of 98.4% and 95.8%. The coefficients of the hydropower production rules of Xin'anjiang Reservoir are shown in Table 4.1.

Table 4.1: Coefficients of the linear hydropower production rules for each zone of Xin'anjiang Reservoir after calibration. The seasons are defined according to the meteorological calendar. Spring thus begins on 1 March, summer on 1 June, autumn on 1 September, and winter on 1 December.

Zone	**Season**	**a [GWh]**	**b [GWh/MCM]**
II	All	11.2	0.0185
III	Spring	−105.8	0.0230
	Summer	−102.6	0.0207
	Autumn	−137.0	0.0245
	Winter	−77.6	0.0197
IV	Spring	6	0.0087
	Summer	0	0.0097
	Autumn	2.5	0.0068
	Winter	20.3	0.0057

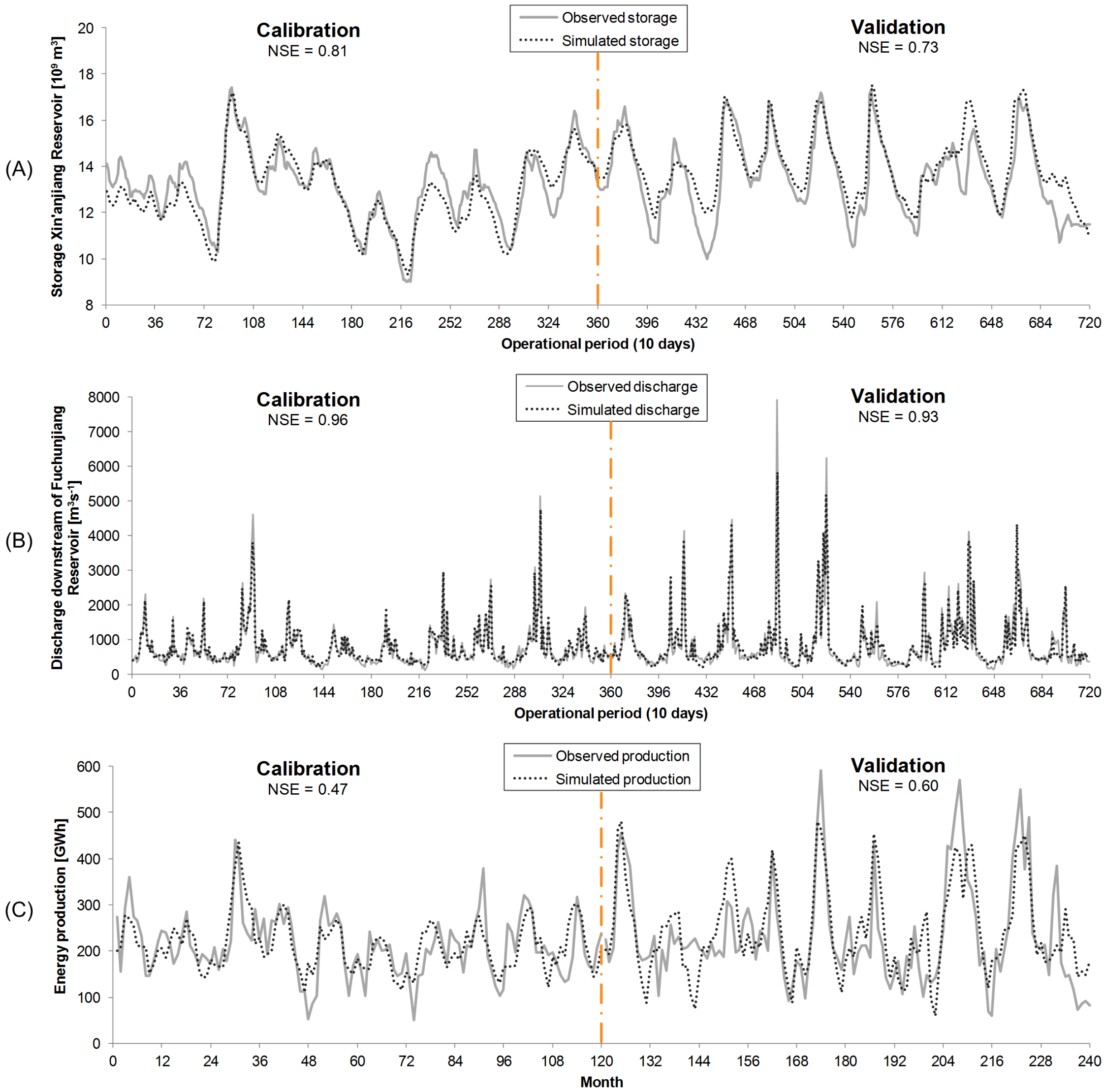

Figure 4.5: Simulation results for the calibration and validation period: 10-day storage volumes of Xin'anjiang Reservoir (A), 10-day discharge directly downstream of Fuchunjiang Reservoir (B) and joint monthly hydropower production of Fuchunjiang Reservoir and Xin'anjiang Reservoir (C).

Calibration resulted in a close fit for the discharge downstream of Fuchunjiang Reservoir and for the storage volumes of Xin'anjiang Reservoir. The monthly cascade hydropower production could however not be simulated with such accuracy (Figure 4.5). This can partially be attributed to the high sensitivity of energy simulations compared to discharge and storage simulations. Energy output is computed according to the equations presented in Appendix C. It involves an efficiency parameter that changes continuously depending on the hydraulic head and on the discharge through the turbines. The model is unable to capture these fluctuations in great detail as it does computations on a 10-day timescale.

Another important aspect is that the model only predicts production levels based on the reservoir storage and inflow. Whenever there is a high energy demand, the operators may decide to produce more energy than would seem logical from a hydrological perspective. Additional errors can be attributed to uncertainties in the inflow forecasts and the human factor in the release decisions. Nevertheless, the accuracy is acceptable for the scope of this study as we intend to use the model for computation of energy production on a longer timescale (annual production totals). The relative error between the observed and simulated Mean Annual Energy Production (MAEP) for the calibration period is +0.5% and for the validation period +5.4%.

4.5 Optimization of reservoir operations

4.5.1 Optimization target parameters

Various authors recognize the potential of coordinated multireservoir operation (Li and Wei, 2008; Liu et al., 2011). Therefore the overall optimization strategy is to reoperate Fuchunjiang Reservoir to a monthly regulating reservoir and to coordinate its operation with that of Xin'anjiang Reservoir. We intend to achieve this coordination by using linear decision rules for both reservoirs. Because of their relative simplicity, linear decision rules are often used in multireservoir operation (Liu et al., 2011; Ostadrahimi et al., 2012). In addition, Karamouz et al. (1992) argued that in most cases more complicated nonlinear decision rules do not yield a significantly higher performance.

The flood control purpose is regarded as a hard constraint to the optimization problem. Therefore the original elevation of the flood control zones of both reservoirs is maintained. Only the release decisions within the conservation pools are subject to optimization. For Xin'anjiang Reservoir, the *conservation pool* comprises the current zones II, III, IV and V (in the optimization considered as a single zone). The conservation pool of Fuchunjiang Reservoir is the fixed zone between 11.6 m+MSL and 24.7 m+MSL (Section 2.3).

We use seasonally varying decision rules in order to discriminate between the different flow regimes of Qiantang River. Variation on smaller time intervals is regarded inappropriate as it drastically increases the amount of optimization parameters, thereby also increasing the likelihood of the algorithm getting stuck in a local optimum. Active storage and inflows of both reservoirs are included in the rules as state variables, with corresponding coefficients to be determined for each season s by the optimization algorithm:

$$E_{X,j} = a_{X,s} + b_{X,s}(S_{a,X,j} + I_{X,j}) + c_{X,s}S_{a,F,j} \tag{4.2}$$

$$E_{F,j} = a_{F,s} + b_{F,s}(S_{a,F,j} + I_{F,j}) + c_{F,s}(S_{a,X,j} + I_{X,j}) \tag{4.3}$$

The total energy production targets E for Xin'anjiang and Fuchunjiang Reservoir (denoted with subscripts X and F respectively) are defined per 10-day operational period j. The production targets are determined by the *active reservoir storage* S_a at the beginning of the current operational period j and forecasted inflow for the current operational period I. Multireservoir coordination is achieved by including the active storage of both cascade reservoirs in the release decision of the individual reservoirs. Additionally the hydropower production of the downstream reservoir is also determined by the inflow to the upstream reservoir.

The goal is to optimize the coefficients of the current linear decision rules of both reservoirs using the NSGA-II algorithm. Since sedimentation is not an issue for either one of the reservoirs (Section 2.1), *flushing* or *sluicing* rules have not been considered in the optimization. In total there are 24 decision variables (six coefficients for each of the four seasons), which are coded in a chromosome structure. We use the *plant factors* and hydropower production efficiencies as obtained by model calibration.

4.5.2 Objective function

Formulation of the optimization objective depends on the specific purpose of the reservoir system under consideration. The Xin'anjiang-Fuchunjiang reservoir cascade has three main purposes:

1. Flood control.
2. Hydropower production.
3. Downstream water supply (water demand and minimum flow requirement).

Downstream flooding and dam overtopping is not allowed within the simulation period. Therefore the flood control purpose is included in the problem formulation as a hard constraint instead of an objective to be minimized. Hydropower production and water supply remain as competing optimization objectives. The results are presented as a tradeoff between these competing objectives, visualized in a *Pareto front*.

Given the current operation style of the reservoir cascade, maximization of the Mean Annual Energy Production (MAEP) is favorable as objective above other criteria such as reliability of power supply. Performance of downstream water supply is expressed as the so called Shortage Index (SI), as defined by the US Army Corps of Engineers (1997). This index reflects the observation that economic and social effects of shortages are roughly proportional to the square of the degree of shortage. The annual SI indicator has been used by various authors and has proven to be highly suitable for reservoir optimization (Chang and Chang, 2009; Tung et al., 2003). In mathematical form the optimization problem can be stated as:

$$max(MAEP) = max\left[\frac{1}{N}\sum_{i=1}^{N}(AEP_i)\right] \tag{4.4}$$

$$min(SI) = min\left[\frac{100}{N}\sum_{i=1}^{N}\left(\frac{D_i}{F_i}\right)^2\right] \tag{4.5}$$

Subject to:

$$\langle D_i, F_i, AEP_i\rangle = WEAP(F_j, I_j, O_j) \tag{4.6}$$

In these equations N is the number of years in the considered study period, D_i is the total deficit in the ith year (supply required minus actual volume supplied) and F_i is the total supply requirement in the ith year. The supply requirement is the sum of water demand and the downstream flow requirement. The Mean Annual Energy Production ($MAEP$) and Annual Energy Production (AEP) are both in GWh. Both indicators are subject to the constraints included in the WEAP model, which simulates with a 10-day timestep j. This model is based on three inputs: F_j, I_j and O_j are the supply requirements, inflows and operating rules in the jth 10-day period, respectively.

Chapter 5

Performance of conventional reservoir operation

In this chapter we evaluate the performance of the Xin'anjiang-Fuchunjiang reservoir cascade using its conventional operating rules. Performance is measured with the Shortage Index (SI) and the Mean Annual Energy Production (MAEP), both introduced in the previous chapter. As a baseline reference, we first investigate the water shortages and energy production for the control period in Section 5.1. Section 5.2 then addresses the performance for each future scenario. In Section 5.3 the actual impact of each scenario is determined by comparing the performance in the control period with the projected future performance.

5.1 Control period

For the control period the water allocation model was employed according to the setup described in Chapter 4. The model does not require a warm-up period as the initial storage levels of both reservoirs, which are normally the only unknowns, could be obtained from historical records. As of January 1, 1971, the total storage volumes of Xin'anjiang Reservoir and Fuchunjiang Reservoir were 10.5 billion m^3 and 0.446 billion m^3, respectively.

An aspect that complicates simulation of the control period is the temporary set of operating rules that were used for Xin'anjiang Reservoir in the period from 1971-1980 (Section 4.4). Since the details of these temporary operating rules are unknown, and in order to make a fair comparison with the future period, the entire control period was simulated as if Xin'anjiang Reservoir was operated with the currently used operating rules.

The results show that there are no significant water shortages in the control period as a Shortage Index of 0.007 was found. This is in line with observations and conclusions of the International Commission on Irrigation and Drainage (Daixin et al., 2005), who confirmed in their study that so far no severe drought events have occurred in the zone downstream of Fuchunjiang Reservoir. Simulations point out that only in 1979 a small *deficit event* occurred. The MAEP of the reservoir cascade in the control period was 2623 GWh.

5.2 Future period

For the future period all scenarios of Chapter 3 were evaluated with the WEAP model. The initial storage volume of Xin'anjiang Reservoir for the future period simulations is unknown. Yet historical records revealed that in the December months between 2001 and 2009 the average pool level was 98.7 m+MSL, equivalent to a storage volume of approximately 12.5 billion m^3. Since there is little fluctuation in storage volume, we assume the same value for the beginning of the future period. As Fuchunjiang Reservoir has a fairly constant pool level, centered around the target storage level of 23 m+MSL, an initial storage of 0.446 billion m^3 was assumed here.

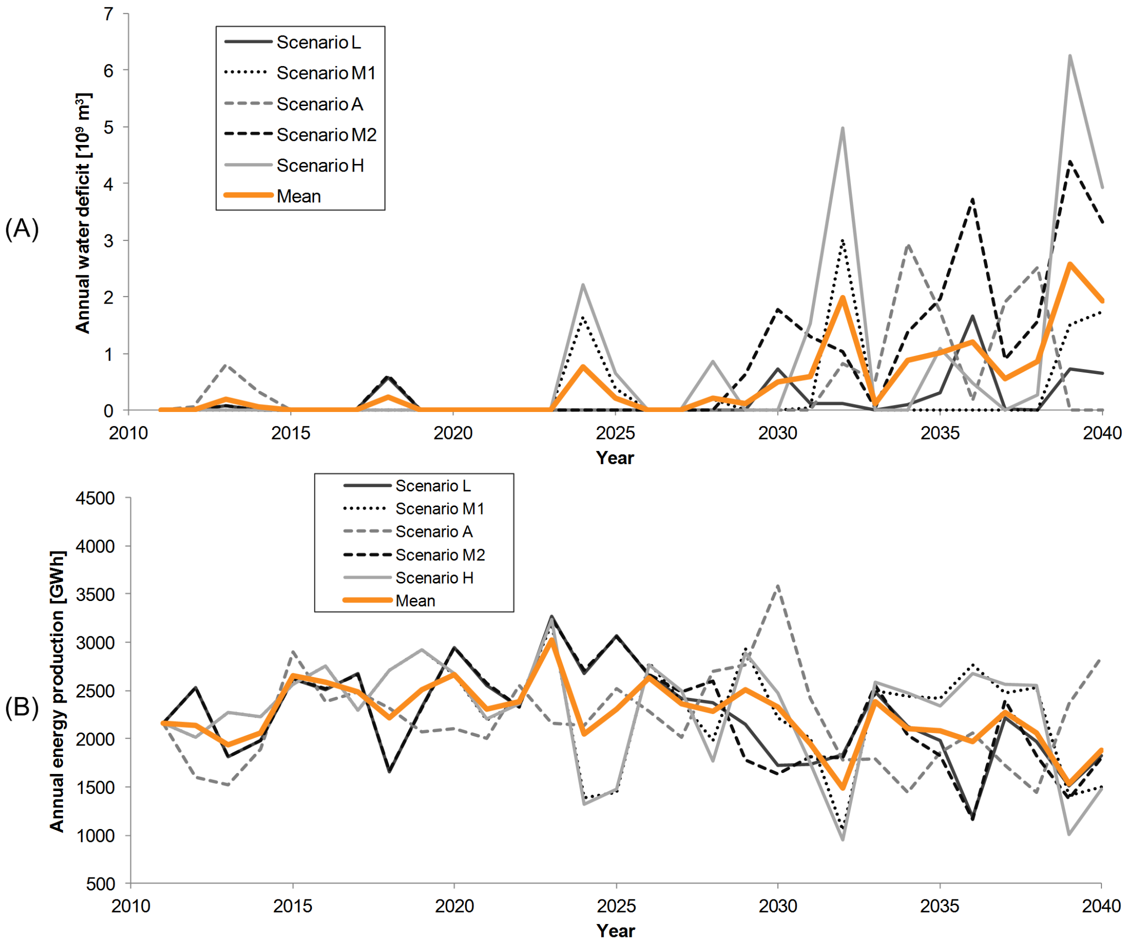

Figure 5.1: Development of the annual water deficit (D) (A) and the Annual Energy Production (AEP) of the reservoir cascade (B) throughout the future period.

The results of the simulations are shown in Figure 5.1 and Table 5.1. Despite the large range of predicted deficits and energy production by the various scenarios, a clear increasing trend is observable for the shortages and a slightly decreasing trend for the energy production. The absolute water deficit rapidly increases after 2030, yet generally remaining low compared to the total supply requirement. A peak deficit of 3.9 billion m^3 is simulated for scenario H in the year 2040, reaching to about 15% of the total supply requirement of that year.

The water shortages considered include both the downstream flow requirement and the *domestic, municipal, industrial* and *agricultural water demand*. Due to the higher allocation priority of the latter categories, most deficits affect the downstream flow requirement only. However, since this automatically leads to significant salt water intrusion and increased pollution levels, it is likely that water intakes close to the river mouth will be paused in such a *deficit event*. Deficits in the downstream flow requirement thus indirectly threaten the continuation of water supply for all other demand categories.

It can be observed that in terms of water shortages, scenario M1 almost has the same impact as scenario A. The water shortages are highest for scenario H and M2, also being the scenarios with the highest projected socio-economic growth. As expected, the lowest SI is found for scenario L. Remarkably, the energy production is highest for scenarios M1 and H, while scenario L shows the lowest energy production. This result is caused by the consistently higher water demand for the H scenario, which forces the reservoirs to release large quantities of water. These releases are then also used to produce additional energy. A negative side effect of this higher production is the systematical decrease in storage volume of Xin'anjiang Reservoir, particularly for scenario H.

Table 5.1: The Shortage Index (SI, dimensionless) and Mean Annual Energy Production (MAEP, in GWh) in each scenario. For comparison also the change in energy production relative to the control period is given between parentheses.

Simulation	**SI**	**MAEP (rel. impact)**
Control period	0.007	2623 (-)
Scenario L	0.05	2243 (-14.5%)
Scenario M1	0.19	2286 (-12.8%)
Scenario A	0.18	2196 (-16.3%)
Scenario M2	0.47	2230 (-15.0%)
Scenario H	0.92	2266 (-13.6%)
Mean future period	0.36	2244 (-14.4%)

5.3 Net performance losses

The impact of each scenario is determined by comparing the SI and MAEP indicators of the future scenarios with the control period. From the results in Table 5.1 it can be observed that the Shortage Index shows an increase from 0.007 in the control period to an average of 0.36 for the future period. Even though this is a large relative increase, the SI is still fairly small when considering the theoretical limits of the index (0 to 100).

The SI is in the same order of magnitude as reported by various other authors, yet somewhat lower than generally found for reservoir systems in China and Taiwan. Yin et al. (2010) for example simulated the performance of a reservoir system in the Tang river basin (China) and reported an SI of 0.4 for the period between 1997 and 2006. Chang and Chang (2009) investigated the current operation of a parallel reservoir system in Taiwan and found SI values between 0.5 and 1.8.

As the SI reflects both the frequency and the magnitude of relative shortages, it must be interpreted likewise (US Army Corps of Engineers, 1997). The SI implies that shortages of 40% are four times as serious as shortages of 20% and that a shortage of 60% would be nine times as costly as a shortage of 20%. There seems not to be a strict consensus in literature as to which SI is still acceptable. According to Gosschalk (2002), an SI in the order of 0.25 is often acceptable (corresponding to a single shortage of 50% in 100 years, or 25 shortage events of 10% each in 100 years). In addition, Chou et al. (2013) evaluated the scheduling of regional water resources projects, using an SI of 0.5 as threshold value for acceptable system performance.

Next to the impact on water shortages, a decrease between -12.8% (scenario M1) and -16.3% (scenario A) is projected for the MAEP in the future period. The mean decrease is -14.4%. This indicates that under conventional operation, a significant impact on energy production is to be expected for all scenarios. Even though the increasing Shortage Index indicates that more drought problems are likely in the future period, the deficits are still fairly small when compared to what is generally regarded acceptable by other authors.

Chapter 6

Reservoir performance after dam reoperation

In this chapter we investigate in how far the impact of socio-economic growth and climate change can be mitigated by coordinated dam reoperation. To this extent we derive operating rules, adapted to each scenario, that minimize the Shortage Index and maximize the Mean Annual Energy Production. In Section 6.1 we present the performance of adapted operating rules per scenario. We also show the relative performance differences compared to conventional operation, which are a scenario-wise measure of impact reduction.

The performance loss that remains after dam reoperation is defined as the residual impact of the projected changes in supply and demand. This impact is measured by comparing the performance after dam reoperation with the historical performance (conventional operation during the control period). The residual impact is presented in Section 6.2, indicating the ability of the reservoir system to adapt to the induced changes in supply and demand. Finally, in Section 6.3, we summarize the findings of this chapter and reflect on the used methodology.

6.1 Impact reduction with adapted operation

According to the setup described in Chapter 4, we search for Pareto-optimal solutions using the NSGA-II *metaheuristic algorithm* interlinked with the WEAP water allocation model. Target parameters for optimization are the three coefficients of the proposed linear hydropower production rules for each of the two reservoirs in the cascade, discriminating between four seasons (24 parameters in total). In total five scenarios for the future period between 2011-2040 were evaluated (30 years per simulation). We also optimize the operations for the control period in order to get some insight in the current optimality of the conventional operating rules.

A well-distributed *Pareto front* was obtained for each optimization of the future period, of which an example is shown in Figure 6.1. Table 6.2 shows the midpoints and edge points of the Pareto fronts obtained for each scenario. The control period optimization yielded a single point as optimum, as the Shortage Index could be completely reduced to zero. The derived coefficients of the hydropower production rules for each scenario are provided in Appendix D.

The actual impact reduction that can be achieved by reoperation is established by a scenario-wise comparison of conventional operation performance (Chapter 5) and adapted operation performance. Compared to conventional operation, the Shortage Index (SI) could be reduced significantly for all future scenarios, while a simultaneous gain in hydropower production was achieved. On average we find a 72% reduction of the SI and a 5.4% gain in Mean Annual Energy Production compared to conventional operation (Table 6.2).

Effects on the SI are larger than reported by other authors, while the hydropower production gains are of a similar order of magnitude. Chang and Chang (2009) for instance reduced the SI of a parallel reservoir system with about 10% after reoperation and a recent study of Fu et al. (2011), which was specifically focused on hydropower production, reported a production gain of about 5%.

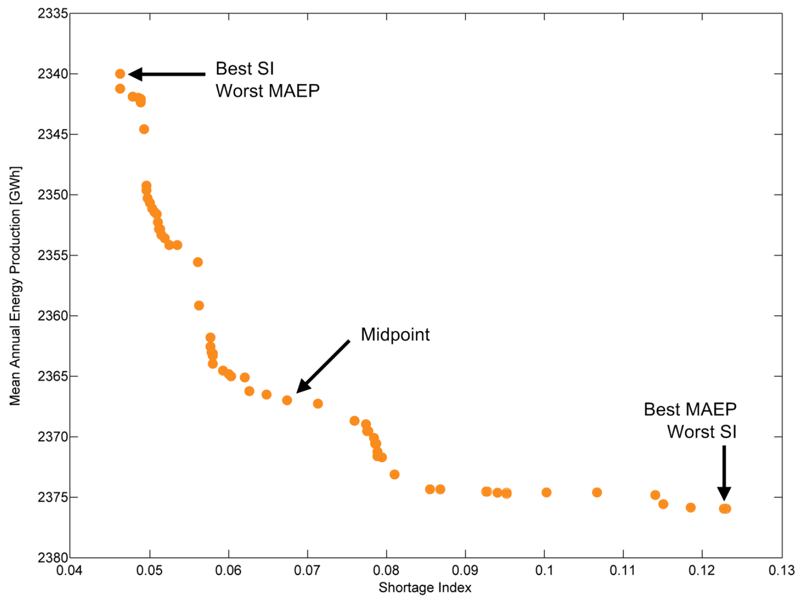

Figure 6.1: Pareto front for the optimization of scenario A after 100 generations. The midpoint is determined by the arc length between the endpoints of the front.)

As explained in Chapter 4, the proposed operating rules enable coordination between both reservoirs. Releases from the upstream Xin'anjiang Reservoir are restricted whenever the storage volume of the downstream Fuchunjiang Reservoir is large. This coordination minimizes unnecessary spills and generally leads to a higher pool level of Xin'anjiang Reservoir (Figure 6.2). A higher pool level leads to additional benefits as it enlarges the effective head on the turbines, resulting in more energy production per unit inflow to the reservoir. A second beneficial aspect of coordination is that we allow for more fluctuations in the pool levels of Fuchunjiang Reservoir, so that more inflow can be buffered and more water can be released through the turbines instead of spillways.

Figure 6.2: Storage volume of Xin'anjiang Reservoir for scenario A. It can be observed that with adapted operating rules the reservoir drawdown is less than conventional operation. The generally higher pool levels ensure a larger head on the turbines, thereby also enabling more hydropower production.

6.2 Residual impact after dam reoperation

Under all investigated future circumstances, reoperation of the Xin'anjiang-Fuchunjiang reservoir system yields a significant impact reduction. In absolute terms however, optimal operating rules are unable to completely restore the system performance to that of the control period. Despite the 5.4% performance gain in hydropower production, the average future decrease is still 9.8% compared to the control period (Table 6.1). Therefore we can state that even though dam reoperation is a highly effective strategy, it cannot be used as a stand-alone solution whenever the goal is to maintain the current performance of the reservoir system.

Table 6.1: The residual impact of each water stress scenario after implementation of adapted operating rules. The residual impact is defined as the difference between the future performance after reoperation and the control period performance of the reservoir system (using conventional operation). Midpoint solutions from the obtained Pareto fronts were selected for this comparison.

Simulation	**Δ SI**	**Δ MAEP [GWh] (rel.)**
Scenario L	+0.002	-259 (-9.9%)
Scenario M1	+0.005	-213 (-8.1%)
Scenario A	+0.060	-256 (-9.8%)
Scenario M2	+0.155	-322 (-12.3%)
Scenario H	+0.248	-236 (-9.0%)
Mean future period	+0.094	-257 (-9.8%)

The residual impact after reoperation is defined as the difference between the future performance after reoperation and the control period performance. Residual performance losses be attributed to the average streamflow in all future scenarios being lower than in the control period. This leads to a reduced average discharge through the reservoir turbines and thus a decrease in hydropower production. The main benefits of adapted operating rules thus lie in their ability to facilitate more extreme variability of the inflow, reducing the amount of spills, enlarging the average head on the turbines and improving the timing of releases.

6.3 Dam reoperation effectiveness

Despite the fact that dam reoperation cannot completely mitigate the impact of climate change and socio-economic developments, it appears to be an elegant strategy to at least reduce the impact. The significant improvements also show that the chosen interlinked simulation-optimization approach is a promising technique to derive optimal operating rules for complex *multireservoir systems*. Even though we have investigated the specific case of *Hangzhou Region*, the methodology can directly be applied to any other water resources system. Yet, the benefits are likely to be dependent on the exact characteristics of the system considered and on the quality of currently used operating rules.

A commonly reported shortcoming of metaheuristic algorithms is a premature convergence of the candidate solutions. This can either be caused by a search space that is too large or by incorrect settings of the algorithm (population size, mutation rate and crossover rate). We experienced that in particular much attention should be paid to restriction of the search space. This has been achieved by determining the range over which each optimization target parameter can fluctuate, such that separate boundary conditions could be applied for each individual parameter. After applying these detailed boundary conditions, we indeed observed fast and consistent convergence to the same optimum.

Table 6.2: The Shortage Index (SI, dimensionless) and Mean Annual Energy Production (MAEP, in GWh) as optimized for each scenario. The impact reduction (performance of adapted operation relative to conventional operation) is shown as a percentage. The edges and center of the Pareto front for each optimization are shown in this table as the worst, midpoint and best result for each objective (the visual interpretation of these definitions are explained in Figure 6.1).

Optimization	**SI (impact reduction)**			**MAEP (impact reduction)**		
	Worst	**Midpoint**	**Best**	**Worst**	**Midpoint**	**Best**
Control period	0 (100%)	0 (100%)	0 (100%)	2802 (6.8%)	2802 (6.8%)	2802 (6.8%)
Scenario L	0.040 (92%)	0.009 (82%)	0 (100%)	2356 (5.0%)	2364 (5.4%)	2372 (5.8%)
Scenario M1	0.061 (68%)	0.012 (94%)	0.009 (95%)	2383 (4.2%)	2410 (5.4%)	2441 (6.8%)
Scenario A	0.120 (33%)	0.067 (63%)	0.046 (74%)	2335 (6.3%)	2367 (7.8%)	2376 (8.2%)
Scenario M2	0.245 (48%)	0.162 (66%)	0.120 (74%)	2251 (0.9%)	2301 (3.2%)	2333 (4.6%)
Scenario H	0.477 (48%)	0.255 (72%)	0.182 (80%)	2336 (3.1%)	2387 (5.3%)	2414 (6.5%)
Mean future period	0.189 (48%)	0.101 (72%)	0.071 (80%)	2332 (3.9%)	2366 (5.4%)	2387 (6.4%)

Chapter 7

Conclusions and recommendations

In the first chapter the objective of this thesis was defined as 'to investigate whether reoperation of the Xin'anjiang-Fuchunjiang reservoir cascade is an effective adaptation strategy to mitigate the potential impacts of climate change and regional socio-economic developments'. The five consecutive research questions were used as a guideline towards this goal. Section 7.1 of this chapter recaps each research question and summarizes the major conclusions. In Section 7.2 recommendations for additional research are provided.

7.1 Conclusions

The design and current operation of the Fuchunjiang-Xin'anjiang reservoir cascade were addressed in Chapter 2, as subject of the first research question. The main finding is that currently both reservoirs are operated individually. Only during potential flood events the operators switch to an emergency control system that coordinates the spillway releases of both reservoirs. Fuchunjiang Reservoir is currently operated as a *Run-Of-River plant*, with only short-term flow regulation ability. However, the reservoir sizing and design suggest that with dam reoperation a regulation ability on longer timescales could be achievable. The larger Xin'anjiang Reservoir has a multiyear flow regulation ability and is operated with linear hydropower production rules that are embedded within five operational storage zones.

Operation of both reservoirs is determined by the incoming streamflow and the water demand of *Hangzhou Region*. The variations herein were investigated on an annual timescale in Chapter 3. The content of this chapter was guided by the second research question, with the goal to identify the likely extent to which climate change and socio-economic developments could impact the future patterns of water supply and demand. The analysis of each separate process resulted in five water stress scenarios for the future period between 2011-2040, which were compared to the control period (1971-2000). Results suggest that there was abundant water available in the control period, which is in line with observations. Yet for all future scenarios there are periods in which the water supply requirements exceed the inflow. There appear to be large seasonal variations in water demand. Particularly the *agricultural water demand* shows large seasonal variations, with a first peak in April and a second peak around July. Despite the regulation ability of the reservoirs in the area, the results indicate that water stress is likely to occur in the future.

All relevant aspects that were explored in Chapters 2 and 3 have been incorporated in the WEAP water allocation model. The modelling setup, described in Chapter 4, involves a simulation module (with WEAP as core component) interlinked with an optimization algorithm. WEAP in itself is capable of simulating water shortages and hydropower production. Since there are large spatial variations in the water demand throughout the study area, each district was assigned a separate water abstraction node in the model. Our optimization strategy involves the NSGA-II *Metaheuristic Algorithm* as core for the optimization module. We adopt linear decision rules in order to achieve coordination of both cascaded reservoirs that are currently operated separately. The Mean Annual Energy Production (MAEP) and Shortage Index (SI) were selected as objective functions.

The actual impact of climate change and socio-economic developments on the performance of the reservoir systems was determined in Chapter 5. We find a Shortage Index of 0.007 for the control period and SI values ranging from 0.05 to 0.92 for the investigated future scenarios. The largest annual deficit is 3.9 billion m^3 (15% of the annual supply requirement), simulated in the high water stress scenario. Even though the increasing SI implies that more drought problems are likely in the future period, the deficits are still fairly small compared to what is generally regarded acceptable in literature. A decrease between -12.8% and -16.3% is projected for the MAEP in the future period, with a scenario-mean decrease of -14.4%. This indicates that under conventional operation, a significant impact on energy production is to be expected for all scenarios.

In Chapter 6 the final research question is addressed regarding the potential of dam reoperation. Based on the optimization results, we conclude that dam reoperation is an effective adaptation strategy to reduce the impact of changing patterns of water supply and demand. Operating rules that are adapted to the forecasted changes result in a significant reduction of the water shortages. Compared to the performance of conventional operation, adapted operating rules reduce the SI by 72% while the MAEP shows an average increase of 5.4%. In absolute terms however, optimal operating rules cannot completely restore the system performance to that of the control period. This is primarily due to the fact that the average inflow in all scenarios is lower than during the control period, leading to a reduced average discharge through the reservoir turbines and thus a decrease in hydropower production. The performance gains for energy production are therefore limited to avoiding unnecessary spills and maintaining an optimal head over the turbines.

Overall we can conclude that, despite the fact that dam reoperation cannot completely mitigate the impact of climate change and socio-economic developments, it appears to be an elegant strategy to at least reduce the impact. The significant improvements also show that the chosen interlinked simulation-optimization approach is a promising technique to derive optimal operating rules for complex *multireservoir systems*. Even though we have investigated the specific case of Hangzhou Region, the methodology can directly be applied to any other water resources system. Yet, the benefits are likely to be dependent on the exact characteristics of the system considered and on the quality of currently used operating rules.

7.2 Recommendations

The conclusions of this study primarily serve a scientific purpose, which is to increase the understanding of dam reoperation potential. However, the findings are also of practical importance since they point out that the water supply of Hangzhou Region can be improved significantly by reoperation of the Xin'anjiang-Fuchunjiang reservoir cascade. Even though the benefits of reoperation are demonstrated by this study, additional studies are necessary before such strategy could actually be implemented.

A first step towards possible implementation is an accurate forecasting of future water demands. In this study we have evaluated various scenarios and shown that for all projected development trajectories reoperation is effective. However, a more detailed long-term forecast of the expected water demands is required to find out which developments are the most likely. In such analysis, also the possibility of more groundwater abstractions (in order to relieve surface water resources) should be investigated. Optimal operating rules for the most likely water demand trajectory can then be selected and tested extensively using additional synthetic discharge series.

The operational consequences for implementation of adapted operating rules is a subject to be investigated in more detail. Adapted rules have consequences for the dispatching of the hydropower plant, dam maintenance schedules, release control systems and the currently used short-term operating rules. Specific analysis of the hydropower dispatching is required, as the derived operating rules only prescribe the optimal dispatching from a hydrological perspective. There may be reasons to deviate from the optimal energy production targets that are related to the demand side of electricity. Additional analysis of the demand side of energy production is therefore recommendable.

From a scientific point of view the importance of this study lies not only in the results but also in the adopted methodology. It has been demonstrated that the chosen simulation-optimization approach is a powerful way to improve reservoir performance. Even though we have selected the NSGA-II genetic algorithm, there is a wide variety of similar *Metaheuristic Algorithms* available. Possible alternatives include Ant Colony Optimization (ACO), Simulated Annealing (SA) and Particle Swarm Optimization (PSO). As there is currently little consensus in literature on the question which of those algorithms delivers the best performance, additional research could reveal the differences between these algorithms in terms of computation speed, convergence characteristics and quality of the results.

Next to the recommendations related to the methodology we can also recommend additional research to verify whether the applied method yields similar benefits for different reservoir systems. Even though the potential benefits of dam reoperation are likely to be determined by the exact characteristics of the water resources system and the performance of its current operation, it is currently unknown which particular characteristics are the most important. As a final aspect, we recognize the uncertainty that lies in the global climate simulations. Therefore it is recommendable to evaluate different Global Circulation Models in addition to the HadCM3 model used in this study.

Bibliography

Anagnostopoulos, J. and Papantonis, D. (2007). Optimal sizing of a run-of-river small hydropower plant. *Energy Conversion and Management*, 48:2663–2670.

Chang, F., Chen, L., and Chang, L. (2005). Optimizing the reservoir operating rule curves by genetic algorithms. *Hydrological Processes*, 19:2277–2289.

Chang, L. and Chang, F. (2001). Intelligent control for modelling of real-time reservoir operation. *Hydrological Processes*, 15:1621–1634.

Chang, L. and Chang, F. (2009). Multi-objective evolutionary algorithm for operating parallel reservoir system. *Journal of Hydrology*, 377:12–30.

Chaves, P. and Chang, F. (2008). Intelligent reservoir operation system based on evolving artificial neural networks. *Advances in Water Resources*, 31:926–936.

Chen, L., McPhee, J., and Yeh, W. (2007). A diversified multiobjective GA for optimizing reservoir rule curves. *Advances in Water Resources*, 30:1082–1093.

Chou, F., Lee, H., and Yeh, W. (2013). Effectivess and Efficiency of Scheduling Regional Water Resources Projects. *Water Resources Management*, 27:665–693.

CNKI (2013). China Economic and Social Statistics Database. Retrieved February 15, 2013, from http://www.cnki.net/.

Daixin, L., Kaipeng, J., Shangfu, K., Fuming, G., and Jiafu, C. (2005). *Water Resources Assessment of Qiantang River Basin, China*. International Commission on Irrigation and Drainage, New Delhi.

Deb, K., Pratap, A., Agarwal, S., and Meyarivan, T. (2002). A Fast and Elitist Multiobjective Genetic Algorithm: NSGA-II. *IEEE Transactions on Evolutionary Computation*, 6:182–197.

Deltares (2013). Ribasim. Retrieved April 8, 2013, from http://www.deltares.nl/en/software/101928/ribasim.

FAO (2012a). CROPWAT. Retrieved March 12, 2013, from http://www.fao.org.

FAO (2012b). Measurement of effective rainfall. Retrieved May 1, 2012, from http://www.fao.org.

Fu, X., Li, A., Wang, L., and Ji, C. (2011). Short-term scheduling of cascade reservoirs using an immune algorithm-based particle swarm optimization. *Computers and Mathematics with Applications*, 62:2463–2471.

Gosschalk, E. (2002). *Reservoir Engineering: Guidelines for Practice.* Thomas Telford, London.

Hamon, W. (1961). Estimating potential evapotranspiration. *Journal, Hydraulics Division, Proceedings of the American Society of Civil Engineers*, 87:107–120.

Hangzhou Bureau of Forestry & Water Conservancy (2008). *Hangzhou Water Resources Bulletin [in Chinese].* Hangzhou Bureau of Forestry and Water Conservancy, Hangzhou.

Hydropower and Water Resources Planning & Design General Institute (2006). *Report on the integrated benefit of Xinanjiang hydropower station and reservoir operation mode.* Beijing.

Ines, A. and Hansen, J. (2006). Bias correction of daily GCM rainfall for crop simulation studies. *Agricultural and Forest Meteorology*, 138:44–53.

IPCC (2007). *Contribution of Working Group II to the Fourth Assessment Report of the Intergovernmental Panel on Climate Change.* Cambridge University Press, Cambridge.

Karamouz, M., Houck, M., and Delleur, J. (1992). Optimization and Simulation of Multiple Reservoir Systems. *Journal of Water Resources Planning and Management*, 118:71–78.

Kumar, D. and Naresh, R. (2007). Efficient real coded genetic algorithm to solve the non-convex hydrothermal scheduling problem. *Electrical Power and Energy Systems*, 29:738–747.

Kumar, D. and Reddy, M. (2007). Multipurpose Reservoir Operation Using Particle Swarm Optimization. *Journal of Water Resources Planning and Management*, 133:192–201.

Labadie, J. (2004). Optimal Operation of Multireservoir Systems: State-of-the-Art Review. *Journal of Water Resources Planning and Management*, 130:93–112.

Leander, R. and Buishand, T. (2007). Resampling of regional climate model output for the simulation of extreme river flows. *Journal of Hydrology*, 332:487–496.

Li, X. and Wei, X. (2008). An Improved Genetic Algorithm-Simulated Annealing Hybrid Algorithm for the Optimization of Multiple Reservoirs. *Water Resources Management*, 22:1031–1049.

Liu, P., Guo, S., Xu, X., and Chen, J. (2011). Derivation of Aggregation-Based Joint Operating Rule Curves for Cascade Hydropower Reservoirs. *Water Resources Management*, 25:3177–3200.

Loucks, D. and Van Beek, E. (2005). *Water Resources Systems Planning and Management.* UNESCO, Turin.

Luke, S. (2012). *Essentials of Metaheuristics.* Lulu, Washington.

Minville, M., Brisette, F., Krau, S., and Leconte, R. (2009). Adaptation to Climate Change in the Management of a Canadian Water-Resources System Exploited for Hydropower. *Water Resources Management*, 23:2965–2986.

Minville, M., Brisette, F., and Leconte, R. (2010). Impacts and Uncertainty of Climate Change on Water Resource Management of the Peribonka River System (Canada). *Journal of Water Resources Planning and Management*, 136:376–385.

Oliveira, R. and Loucks, D. (1997). Operating rules for multireservoir systems. *Water Resources Research*, 33:839–852.

Ostadrahimi, L., Marino, M., and Afshar, A. (2012). Multi-reservoir Operation Rules: Multi-swarm PSO-based Optimization Approach. *Water Resources Management*, 26:407–427.

Pan, X., Geng, Y., Zhang, W., Li, B., and Chen, J. (2006). The influence of abiotic stress and phenotypic plasticity on the distribution of invasive Alternanthera philoxeroides along a riparian zone. *Acta Oecologica*, 30:333–341.

Payne, J., Wood, A., Hamlet, A., Palmer, R., and Lettenmaier, D. (2004). Mitigating the effects of climate change on the water resources of the Columbia river basin. *Climatic Change*, 62:233–256.

Perrin, C., Michel, C., and Andréassian, V. (2003). Improvement of a parsimonious model for streamflow simulation. *Journal of Hydrology*, 279:275â“289.

Qiu, J., Tang, H., Frolking, S., Boles, S., Li, C., Xiao, X., Liu, J., Zhuang, Y., and Qin, X. (2003). Mapping Single-, Double-, and Triple-crop Agriculture in China at 0.5○ x 0.5○ by Combining County-scale Census Data with a Remote Sensing-derived Land Cover Map. *Geocarto International*, 18:3–13.

Raje, D. and Mujumdar, P. (2010). Reservoir performance under uncertainty in hydrologic impacts of climate change. *Advances in Water Resources*, 33:312–326.

Rani, D. and Moreira, M. (2010). Simulation-Optimization Modeling: A Survey and Potential Application in Reservoir Systems Operation. *Water Resources Management*, 24:1107–1138.

Salazar, D., Rocco, C., and Galván, B. (2006). Optimization of constrained multiple-objective reliability problems using evolutionary algorithms. *Reliability Engineering and System Safety*, 91:1057–1070.

Schumann, A. (1995). Flexibility and adjustability of reservoir operation as an aid for sustainable water management. In *Modelling and Management of Sustainable Basin-scale Water Resource Systems*, pages 291–297.

SEI (2013). WEAP: Water Evaluation And Planning system. Retrieved April 8, 2013, from http://www.sei-international.org/weap-the-water-evaluation-and-planning-system/.

Terink, W., Hurkmans, R., Torfs, P., and Uijlenhoet, R. (2009). Bias correction of temperature and precipitation data for regional climate model application to the Rhine basin. *Hydrology and Earth System Sciences Discussions*, 6:5377–5413.

The World Bank (2013). GDP deflator. Retrieved January 16, 2013, from http://data.worldbank.org.

Tung, C., Hsu, S., Liu, C., and Li, S. (2003). Application of the genetic algorithm for optimizing operation rules of the LiYuTan Reservoir in Taiwan. *Journal of the American Water Resources Association*, 39:649–657.

US Army Corps of Engineers (1997). Hydrologic Engineering Requirements for Reservoirs. Retrieved May 5, 2012, from http://publications.usace.army.mil.

US Army Corps of Engineers (2013). HEC-ResSim. Retrieved April 8, 2013, from http://www.hec.usace.army.mil/software/hec-ressim/.

Vörösmarty, C., Green, P., Salisbury, J., and Lammers, R. (2000). Global Water Resources: Vulnerability from Climate Change and Population Growth. *Science*, 289:284–288.

Wada, Y., Van Beek, L., Viviroli, D., Dürr, H., Weingartner, R., and Bierkens, M. (2011). Global monthly water stress: 2. Water demand and severity of water stress. *Water Resources Research*, 47:WO7518.

Wang, Q., Zhang, S., and Ho, E. (2010). The China Files: Chinese Economy through 2020. Retrieved January 15, 2013, from http://www.morganstanley.com.

Wang, X., Fan, G., and Liu, P. (2007). Pattern and Sustainability of China's Economic Growth towards 2020. Retrieved January 15, 2013, from http://draft.cerdi.org/.

Wurbs, R. (2003). Reservoir-system simulation and optimization models. *Journal of Water Resources Planning and Management*, 119:455–472.

Yin, X., Yang, Z., Yang, W., Zhao, Y., and Chen, H. (2010). Optimized reservoir operation to balance human and riverine ecosystem needs: model development, and a case study for the Tanghe reservoir, Tang river basin, China. *Hydrological Processes*, 24:461–471.

Zhejiang Design Institute of Water Conservancy & Hydroelectric Power (2006). *Case study to the Water Supply from Xinanjiang Reservoir [in Chinese]*. Zhejiang Design Institute of Water Conservancy & Hydroelectric Power, Hangzhou.

Zhejiang Design Institute of Water Conservancy & Hydroelectric Power and Zhejiang Institute of Hydraulics & Estuary (2005). *Report on the Planning and Allocation of Water Resources in Qiantang River [in Chinese]*. Zhejiang Design Institute of Water Conservancy & Hydroelectric Power and Zhejiang Institute of Hydraulics & Estuary, Hangzhou.

Appendices

Appendix A

Hydrology in detail

This appendix addresses the hydrology of the study area from a more detailed point of view. A summary of the regional climate and properties of the various river sections in the study area is provided in Section A.1. In Section A.2 the available data is discussed, along with the actual implementation in the WEAP model.

A.1 Hydrological area characteristics

Qiantang River Basin has a sub-tropical monsoon climate with four distinct seasons. The average annual precipitation is between 1200 mm and 2200 mm. It is strongly correlated to the land surface topography: the mountainous areas generally have more precipitation than the plains. Annual evaporation rates are between 800 mm and 1000 mm. The evaporation is highest in the coastal areas and lowest in the mountains. The average annual temperature ranges from 16°C to 18°C (Daixin et al., 2005).

Table A.1: Hydrological characteristics of the relevant river sections. Length and catchment area of each section includes its child sections.

River section	**Mean discharge** [m^3s^{-1}]	**Area** [km^2]	**Length** [km]	**Parent section**
Lan River	543	19,468	303	Fuchun River
Xin'an River	335	11,674	359	Fuchun River
Fenshui River	90	3,444	165	Fuchun River
Fuchun River	968	38,318	461	Qiantang River
Puyang River	75	3,452	150	Qiantang River
Qiantang River	1043	55,558	605	-

Qiantang river has several large tributaries. Most of the water flows into Hangzhou Region through Lan River and Xin'an River, who originate in mountainous areas and confluence in the center of the catchment. From this confluence point the river continues as the Fuchun River. Smaller tributaries, Fenshui River and Puyang River, flow into this main branch. At the confluence point with the latter, just before entering Hangzhou City, the name becomes Qiantang River. The main hydrological characteristics of each branch are summarized in Table A.1.

A.2 Available data and model implementation

There are seven relevant hydrological fluxes going in and out of the study area. This section described how the datasets were obtained and preprocessed.

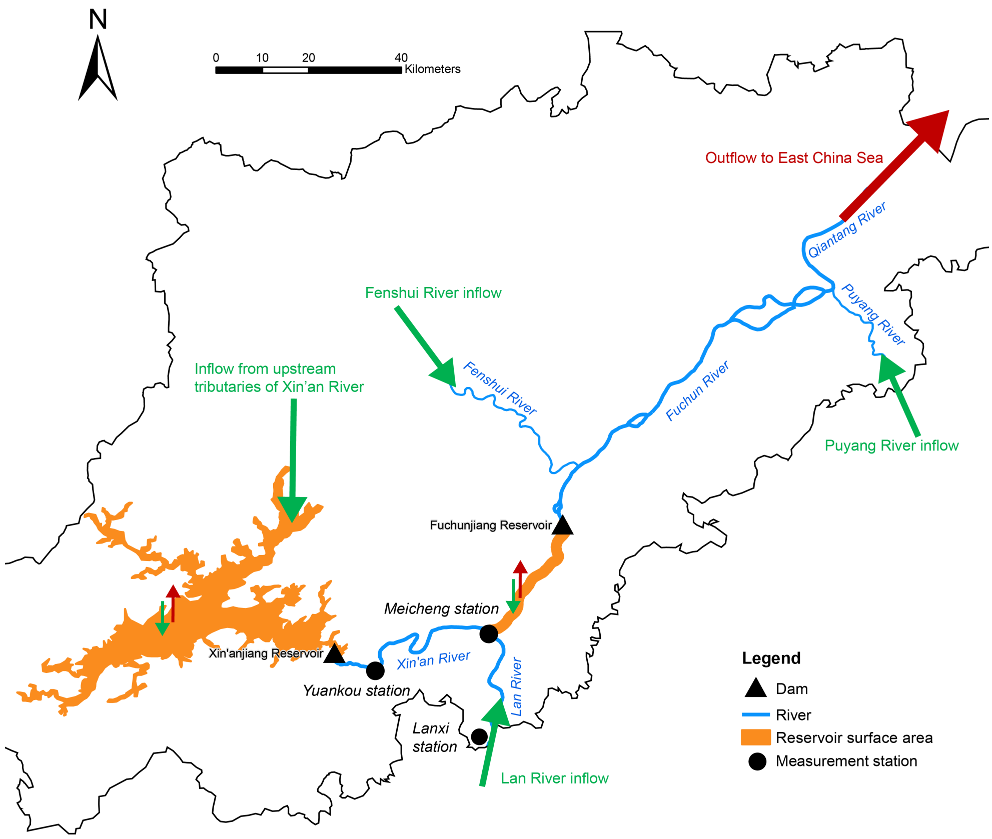

Figure A.1: Overview of all relevant hydrological fluxes going in (green arrows) and out (red arrows) of the study area.

A.2.1 Inflow from Lan River

Discharge from the Lan River branch is recorded at the Lanxi discharge station. The original dataset was in daily timesteps, from 1971 till 2000. The data was aggregated to 10-day timesteps, thereby considering historical leap years. The inflow was implemented in the WEAP model as a so called headflow property for the Lan River link. Streamflow for the future scenarios was simulated on daily basis with the GR4J model. Output of this model was also aggregated to 10-day periods and then fed into the WEAP model.

The accuracy of future discharge predictions is subjected to some uncertainty caused by upstream anthropogenic activities. The first source of uncertainty is the extent to which the amount of water abstractions upstream of Lanxi station are to change in the future. A significant increase in water withdrawal in upstream branches is not accounted for in the hydrological simulations, as the GR4J model is calibrated based on the current outflows of the entire subbasin. Increasing upstream abstractions due to population growth and increasing economic activity would likely result in a slightly lower discharge than is currently predicted.

A second aspect is the various Run-Of-River hydropower stations that are present along the upstream branches of Lan River. These dams will in reality influence the natural discharge patterns of the river. However, as they have no significant flow regulation ability, the influence on 10-day aggregated discharge is assumed to be neglectable.

A.2.2 Inflow from tributaries of Xin'an River

The outflow from the Xin'an subbasin is nowadays completely regulated by Xin'anjiang Reservoir. As the inflow to this reservoir comes from a large number of smaller tributaries, it was not possible to obtain direct discharge records. Therefore the inflow was reconstructed based on historical reservoir storage levels, historical releases and net precipitation on the reservoir. The inflow is specified as a single link in WEAP, representing all tributaries together. The GR4J model was used for simulation of streamflow in the future period.

A.2.3 Evaporation and precipitation

Detailed pan evaporation measurements (E601) were obtained for the period 1981-1990. The measurements are from Yuankou station, located downstream of Xin'anjiang Dam (close to Jiande City). The original pan evaporation measurements have been converted to lake evaporation using monthly pan coefficients.

Daily precipitation measurements were obtained from Meicheng station, located at the bifurcation point of Lan River and Xin'an River. The original dataset covered the period 1961-2000. The first 10 years were omitted in further calculations. The stations are assumed to be representative for the evaporation and precipitation on both reservoirs.

The evaporation and precipitation fluxes were aggregated into 10-day timesteps and averaged for the simulation period. They were included in WEAP as a net evaporation flux to estimate reservoir system losses (for both Xin'anjiang Reservoir and Fuchunjiang Reservoir).

Table A.2: Precipitation (P), reference evapotranspiration (ET_0) and simplified discharge of Fenshui and Puyang River as implemented in WEAP.

Month	**P** [mm d^{-1}]	**ET_0** [mm d^{-1}]	**Discharge [m^3 s^{-1}]** Fenshui River	Puyang River
Jan	1.95	0.82	30	50
Feb	2.97	0.80	65	63
Mar	4.64	0.99	115	75
Apr	5.46	1.72	126	88
May	5.38	2.44	145	100
Jun	7.97	2.61	192	113
Jul	4.7	3.69	126	100
Aug	4.15	4.09	91	88
Sep	2.98	2.8	90	75
Oct	2.16	2.09	48	63
Nov	1.62	1.53	36	50
Dec	1.27	1.11	24	38

A.2.4 Groundwater fluxes

Groundwater fluxes along the boundaries of the study area are assumed to be insignificant compared to the total discharge of Qiantang River. Seepage losses that occur from Xin'anjiang Reservoir have been monitored in recent years. The total seepage through the dam and ground appears to be 0.0015 m^3 s^{-1}, which is neglectable.

A.2.5 Inflow from Fenshui River

The discharge of Fenshui River is controlled by Fenshui Hydro Junction, a small reservoir that maintains a fairly constant outflow. The average discharge is about 90 m^3 s^{-1}, which is only 9% of the total discharge of Qiantang River. The monthly average discharges were obtained from the Hangzhou Water Resources Bulletin (Hangzhou Bureau of Forestry & Water Conservancy, 2008), shown in Table A.2.

A.2.6 Inflow from Puyang River

Puyang River is the furthest downstream tributary of Qiantang River. It is fairly small, with an average flow of 75.5 m^3 s^{-1} (Hangzhou Bureau of Forestry & Water Conservancy, 2008). According to Pan et al. (2006), the discharge varies from about 1.5 times the average in the wet season to as low as 0.5 times the average in the dry season. No long-term discharge records were available for Puyang River, but the small streamflow (about 7% of the total discharge of Qiantang River) justifies a more simplified implementation in the model (Table A.2).

Appendix B

Water demand in detail

As discussed in Chapter 3, a total of four water demand categories are considered in this study: domestic (rural and urban), municipal, industrial and agricultural (irrigation and livestock/fishery) demand. The water demand for these categories is computed separately for each of the five districts in the study area, represented by a withdrawal node in the WEAP model. Section B.1 presents the unit demand rates and consumption rates for each category and per district. As only annually aggregated water demand could be obtained from literature, the seasonal variations herein have been estimated. The related computational procedures are explained in Section B.2.

B.1 Unit demand and consumption rates

Actual water demands, population numbers and irrigated farmland were obtained from the Hangzhou Water Resources Bulleting (Hangzhou Bureau of Forestry & Water Conservancy, 2008). The nominal *industrial output* was obtained from the China Economic and Social Statistics Database and corrected with inflation data (The World Bank, 2013). Based on these statistics, the actual unit demand rates have been calculated. The resulting rates are shown in Table B.1.

Table B.1: Unit demand rates.

Demand category	**Demand rate**					**Unit**	**Cons. rate [%]**
	Hangzhou (urban)	**Fuyang**	**Tonglu**	**Jiande**	**Chun'an**		
Domestic (urban)	66	75	46	83	34	m^3/cap/yr	36.9
Domestic (rural)	41	39	41	54	61	m^3/cap/yr	84.2
Municipal	263.1	110.6	18.6	17.3	14.7	m^3/cap/yr	52.1
Industrial	6.60	2.55	0.47	0.47	0.23	MCM/10^9 RMB/yr	32.5
Agricultural (irrigation)	0.78	0.78	0.89	0.89	1.30	MCM/km^2/yr	75.3
Agricultural (fishery and livestock)	220.3	47.8	128.1	30.6	14	m^3/cap/yr	86.2

We have accounted for the fact that only a portion of the water demand is actually consumed, and the remaining part will be returned to the system after usage. The amount of water demand that is withdrawn from the system is expressed as the so called consumption rate. This rate has been obtained from the Hangzhou Water Resources Bulletin (Hangzhou Bureau of Forestry & Water Conservancy, 2008) and is specified uniquely for each separate demand category (Table B.1).

B.2 Seasonal variations in water demand

B.2.1 Domestic demand

It has been assumed that municipal and industrial water demand remain constant throughout the year. Variation in water demand for domestic purposes is estimated as a function of temperature (Wada et al., 2011). To this extent we use the monthly averaged temperature for Hangzhou Region. Water demand variations are computed as follows:

$$C_{d,m} = \frac{C_{d,i}}{12}\left[\left(\frac{T_m - T_{m,avg}}{T_{max} - T_{min}} r\right) + 1.0\right] \tag{B.1}$$

In this equation $C_{d,m}$ is the domestic demand in month m, $C_{d,i}$ the total domestic demand in year i, T_m the actual temperature, $T_{m,avg}$ the average monthly temperature and T_{max} T_{min} the maximum and minimum temperature, respectively (all in $°C$). The constant r is the dimensionless amplitude, representing the relative difference between the domestic water demand in the warmest and the coldest month. A value of 0.1 was used in this study, as it appears to fit well with observed variations in areas with a similar climate as Hangzhou Region (Wada et al., 2011).

B.2.2 Irrigation demand

Monthly variations in irrigation water demand are estimated using the CROPWAT method. Based on the dominant crop types, a simplified representation of the area was made. Hereby the five prevailing crop rotation schemes are considered: rice/winter wheat, potato/vegetable, rapeseed/winter wheat and vegetable/winter wheat (Qiu et al., 2003). The approximate area used for each crop calendar was obtained from the China Economic and Social Statistics Database (CNKI, 2013). In total, the five considered rotations covered about 2690 km^2, which is 71% of the total cultivated area.

Based on the situation in 2010, rice/winter wheat was the predominant calendar, covering about 30% of the considered farmland. Approximately 24% was used for potato/vegetable, 19% for maize/winter wheat, 14% for rapeseed/winter wheat and 12% for vegetable/winter wheat. The considered crops are generally speaking located in irrigated areas. It has been assumed that the crop patterns have not significantly changed throughout the years.

The irrigation demand C_{irr} for each crop type is computed with the following equation:

$$C_{irr} = E_p - P_e \tag{B.2}$$

In this equation E_p is the potential crop evapotranspiration (mm/day) and P_e the effective rainfall in mm/day. The effective rainfall is defined as the part of the rainfall which is effectively used by the crop after rainfall losses due to surface run off and deep percolation have been accounted for.

Table B.2: Key input values for the CROPWAT calculations: crop coefficients K_c and land preparation dose. The table also reflects the different planting dates of the crop types. Rice requires a large initial preparation dose as the land is flooded after sowing.

Month				$\mathbf{K_c}$ **[-]**				**Land prep. dose [mm]**
	Rice	**Winter wheat**	**Potato**	**Vegetables (autumn sown)**	**Vegetables (spring sown)**	**Rapeseed**	**Maize**	
Jan	0	1.15	0	1.05	0	0	0	0
Feb	0	1.15	0	0.75	0	0	0	0
Mar	0	0.75	0	0	0	0	0	0
Apr	1.10	0.30	0.50	0	0.78	0.35	0	200 (rice)
May	1.19	0	1.15	0	0.95	1.15	1.20	0
Jun	1.20	0	1.15	0	1.05	1.15	1.20	0
Jul	1.20	0	0.90	0	1.05	1.75	1.00	0
Aug	1.10	0	0.65	0	0.75	0.35	0.50	0
Sep	1.10	0	0	0	0	0	0	0
Oct	0	0	0	0.78	0	0	0	0
Nov	0	0.70	0	0.95	0	0	0	0
Dec	0	1.00	0	1.05	0	0	0	0

Based on the recommendations of FAO (2012b), a constant rainfall effectiveness of 80% was assumed. Average precipitation from Table A.2 was used in the calculations. The potential crop evapotranspiration is computed as follows:

$$E_p = K_c ET_0 \tag{B.3}$$

Here K_c is the crop coefficient (dimensionless) and ET_0 the reference evapotranspiration (mm/day). The average irrigation demand per unit land area was determined by computing the irrigation demand for each crop type and multiplying this with its respective relative land cover.

B.2.3 Resulting seasonal pattern

Based on the methods presented in the previous subsections, we obtain the seasonal demand variations shown in Figure B.1.

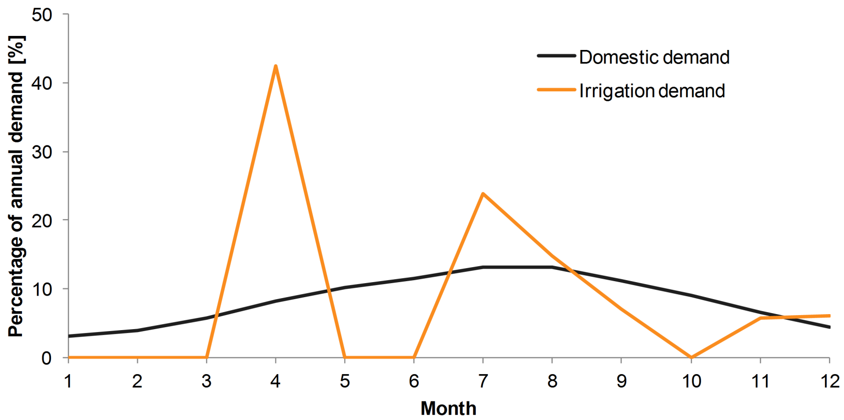

Figure B.1: Seasonal demand variations.

Appendix C

Reservoir operations in detail

In this appendix the details behind reservoir operation are addressed. Section C.1 explains the physical constraints to reservoir operation from a theoretical point of view and discusses the implementation of these constraints in the WEAP model. In Section C.2 hydropower operations are discussed, along with their model implementation. The allocation priority of the various supply targets is subject of Section C.3.

C.1 Physical reservoir constraints

Under normal circumstances, water is released from a reservoir through penstocks in the dam that lead to the powerhouse. Whenever more discharge capacity is needed, spillways can be enabled. *Spillways* are hydraulic structures that are normally used during flood events, in order to prevent overtopping or damaging of the dam. Opening of spillways is however not favorable as the spilled water cannot be used to generate hydropower.

C.1.1 Background

The change in storage of a reservoir during a certain time period t can be described by a simple water balance equation:

$$\Delta S_t = I_t + P_{H,t} - G_{H,t} - R_{H,I,F,t} - E_{H,t} \quad \text{(C.1)}$$

In this equation ΔS is the change in storage (m^3), determined by the total inflow I, precipitation P, groundwater seepage G, reservoir releases R and evaporation E (all in m^3). Most variables in this equation are variable in time, but also depend on the pool level H of the reservoir. The surface area also increases with the pool level, thus affecting precipitation and evaporation fluxes. Head differences also affect the seepage from the reservoir. Reservoir releases are a function of head, inflow, downstream supply requirements F and time.

Release rules generally prescribe the amount of water to be released depending on inflow, reservoir storage and demand. The total releases are constrained by the maximum hydraulic outflow Q_{max}:

$$R \leq Q_{max}(H) \quad \text{(C.2)}$$

The maximum hydraulic outflow is determined by both the water level in the reservoir at a certain timestep and by the capacity of the various dam components. Whenever the *pool level* is below the penstock intakes, no outflow is possible. For pool levels between the spillway crest and the penstocks, the total penstock capacity can be utilized to discharge water.

Whenever the pool level is above the spillway crest, the outflow depends on the operation of the *spillway*, the pool level, and the hydraulic constraints of the spillways. This together is defined in a so called spillway head-discharge relation. Finally, for pool levels above the dam crest, overtopping will occur. In that case, the maximum flow is virtually unlimited (even though in reality still bounded by friction).

In mathematical form, the maximum hydraulic outflow Q_{max} can be defined as:

$$Q_{max} = \begin{cases} 0 & \text{if } H < h_p \\ Q_{p,max} & \text{if } h_p < H < h_s \\ Q_{p,max} + Q_s(h) & \text{if } h_s < H < h_c \\ \infty & \text{if } H > h_c \end{cases} \quad \text{(C.3)}$$

In this equation H is the pool level, h_p the penstock intake level, h_s the spillway crest level and h_c the dam crest level (all in meters). The total penstock capacity $Q_{p,max}$ and spillway discharge Q_s are in m s^{-1}.

C.1.2 Model implementation

Storage-elevation tables were obtained for both reservoirs in order to compute reservoir pool levels as a function of current storage. The obtained data is shown in Figure C.1.

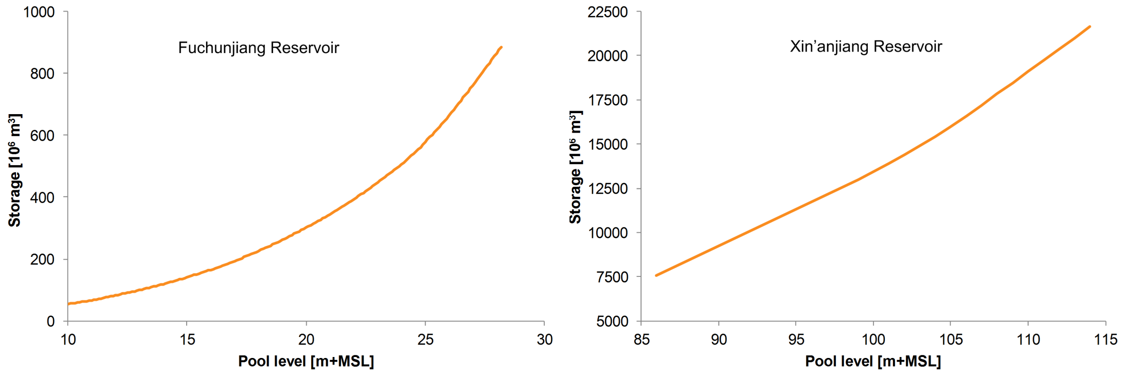

Figure C.1: Storage elevation curves for both reservoirs.

WEAP uses two variables to define total reservoir release constraints. The first one is the *Maximum Hydraulic Outflow* (Q_{max}), which is the total amount of water that can be discharged from the reservoir at a certain water level. The second variable is the Maximum Turbine Flow $Q_{p,max}$, which is the maximum amount of water that can be discharged through the penstocks at a given water level. WEAP will not release water if the reservoir storage is equal or lower than the *dead storage*.

Spillway head-discharge relations have also been obtained with fourth-order regression, based on existing tabulated data:

$$Q_{s,k} = s_k H_{k,t}^4 + u_k H_{k,t}^3 + v_k H_{k,t}^2 + w_k H_{k,t} + z_k \quad \text{(C.4)}$$

In this equation s, u, v, w and z are regression coefficients, obtained for each reservoir k. The maximum spillway flow Q_s in each timestep t is in m^{3}s^{-1}.

Table C.1: Release constraint settings in WEAP.

Parameter [unit]	**Xin'anjiang Reservoir**	**Fuchunjiang Reservoir**
h_s [m+MSL]	99	11.6
h_p [m+MSL]	70.4	15
$Q_{p,max}$ [m^{3}s^{-1}]	1291.5	1300
S_{tot} [10^6 m^3]	21626	554.30
s	-0.03198	0
u	11.67	-0.1885
v	-1510	15.87
w	8.001×10^4	-279.2
z	-1.375×10^6	1403

C.2 Hydropower operations

C.2.1 Background

The powerhouse of a dam usually contains several turbine units and generators. The power production is however bound by several constraints. Firstly, the generated electric power can never exceed the *installed capacity* P_j^C. This capacity, also called *nameplate capacity*, is the technical upper limit of power output.

$$P_j \leq P_j^C \tag{C.5}$$

Second important limitation is that the turbines only work above a minimum net head and only if there is sufficient flow. Furthermore, the net head over the turbines cannot exceed a specified maximum to prevent damage to the equipment. Within the boundaries of these constraints the generated electric power P (in W) for each operating unit j is obtained from the general hydropower equation (Anagnostopoulos and Papantonis, 2007):

$$P_j = \begin{cases} 0 & \text{if } h_{net} < h_{min} \\ \rho g h_{net}(t) \eta_j Q_j(t) & \text{if } h_{max} < h_{net} > h_{min} \\ 0 & \text{if } h_{net} > h_{max} \end{cases} \tag{C.6}$$

where ρ is the density of water (1000 kg m^{-3}), g the gravitational acceleration (9.81 m s^{-2}), h_{net} the net head over the turbines in m, Q the discharge through the turbines in m^3/s and η is the overall efficiency (dimensionless). The overall efficiency is the product of efficiencies of the hydraulic turbine, the electrical generator and the transformer. It depends on the quality of these components, but also on the net head and the turbine flow. Most dams use advanced flow allocation systems that maintain a high efficiency by disabling certain turbines when low energy is produced. Therefore in practice the actual efficiency is fairly constant and in this study assumed to be independent of net head and total flow.

The net head in equation C.2.1 is the head available at the inlet of the turbine. It can be computed by subtracting the hydraulic losses due to penstock friction from the gross head. This gross head is defined as the difference between reservoir pool level and the tailwater level when no water is flowing. In mathematical form:

$$h_{net}(t) = H(t) - h(t) - h_f \tag{C.7}$$

In which $H(t)$ is the reservoir *pool level* and $h(t)$ the *tailwater level*, both in m+MSL. The hydraulic losses h_f (in m) depend on the relative roughness of the penstock material and the bends and curves in the piping.

The tailwater level at the toe of both dams is determined by the releases from the reservoir. In theory, the pool level of Fuchunjiang Reservoir could also influence the tailwater level of Xin'anjiang Reservoir. Yet, this requires unusually high water that do not occur frequently. Therefore it has been assumed that the tailwater level of Xin'anjiang Reservoir is independent of the operation of Fuchunjiang Reservoir.

C.2.2 Implementation

WEAP has no build-in functionality to determine the net head over a turbine. It only calculates the gross head and uses this as input for its hydropower calculations. Therefore the hydraulic loss has been added in WEAP as an auxiliary parameter, which is added to the tailwater level in each timestep, thereby effectively lowering the head of the turbines to the approximate net head.

For the hydropower production WEAP uses a so called *plant factor*, which is defined as the fraction of each timestep that water is released while the power plant is online. This definition is different from the aforementioned *plant load factor*, which is the ratio between amount of energy produced divided by the *installed capacity.* The plant factor is usually larger than 95%, as a plant is normally offline only for critical maintainance works to the generators. Often only a small part of all turbine/generator units is unavailable, such that the plant can keep generating at all times.

The relation between reservoir releases and corresponding tailwater level has been determined by fourth-order regression of historical water level and discharge measurements. In a general form the tailwater level h of reservoir k (in m+MSL) is given by:

$$h_{k,t} = a_k R_{k,t}^4 + b_k R_{k,t}^3 + c_k R_{k,t}^2 + d_k R_{k,t} + e_k \tag{C.8}$$

In which a, b, c, d and e are regression coefficients, obtained for each reservoir k. The releases R in each timestep t are in m^3s^{-1}.

Table C.2: Hydropower parameter settings in WEAP.

Parameter [unit]	**Xin'anjiang Reservoir**	**Fuchunjiang Reservoir**
h_{max} [m]	80	-
h_{min} [m]	57.8	-
h_f [m]	0.3	0.2
a	0	-4.355×10^{-16}
b	1.077×10^{-9}	1.534×10^{-11}
c	-3.284×10^{-6}	-2.082×10^{-7}
d	5.530×10^{-3}	1.746×10^{-3}
e	22.61	5.421

C.3 Allocation priorities

WEAP uses an internal linear solver to allocate water based on the actual demand, supply and the allocation priority. The prioritization of the model is based on existing studies (Hydropower and Water Resources Planning & Design General Institute, 2006) and interviews with dam operators:

1. Hydropower production Xin'anjiang Reservoir.
2. Hydropower production Fuchunjiang Reservoir.
3. Water demand (equal for all demand nodes and categories herein).
4. Downstream flow requirement.
5. Refill of Xin'anjiang Reservoir.
6. Refill of Fuchunjiang Reservoir.

The reservoir cascade is primarily operated for hydropower production. Downstream water demand therefore has a relatively low priority. In case of a severe *deficit event*, water is only released to meet hydropower production targets. In case those releases are insufficient to satisfy downstream water demand, the downstream flow requirement is determined to be the first unmet allocation target.

Hydropower production and refills of Xin'anjiang Reservoir have a higher priority than Fuchunjiang Reservoir since the operators of the Xin'anjiang Reservoir do not consider downstream hydropower production targets in their release decisions. Under normal operation, when there is abundant water, this prioritization makes no difference as both reservoirs can achieve their production targets. During periods of drought however, the higher priority of Xin'anjiang Reservoir will prevent additional releases that are required for the sole benefit of Fuchunjiang Reservoir.

Appendix D

Adapted operating rules

A direct Parameterization-Simulation-Optimization (PSO) approach was used to derive optimal operating rules for each water stress scenario. The optimized coefficients for the hydropower production rules (Section 4.5) are presented in this appendix. Performance of the adapted rules is presented in Chapter 6.

Table D.1: Coefficients of the adapted linear hydropower production rules. The coefficients for each scenario yield a fitness that corresponds to the midpoint of the respective Pareto front. Coefficient a is in GWh, b and c are in GWh/MCM.

Simulation	**Season**	a_X	b_X	c_X	a_F	b_F	c_F
Control period	Spring	2.5	0.0121	-0.0150	3.5	-0.0130	-0.0033
	Summer	7.4	0.0010	-0.0063	0	-0.0120	-0.0100
	Autumn	40	0.0032	0.0032	0	-0.0053	-0.0028
	Winter	11.7	0.0085	0.0047	0.3	-0.0135	-0.0007
Scenario L	Spring	14.3	0.0075	0.0008	5.1	-0.0086	-0.0069
	Summer	9.6	0.0043	-0.0110	4.8	-0.0054	-0.0067
	Autumn	33.5	0.0026	-0.0055	5.1	-0.0137	0.0014
	Winter	17.3	0.0073	0.0011	1.8	-0.0177	-0.0006
Scenario M1	Spring	30	0.0029	0.0020	6.2	0.0007	-0.0021
	Summer	11.2	0.0033	-0.0072	3.7	-0.0048	-0.0020
	Autumn	34.7	0.0020	-0.0051	0	-0.0147	0.0006
	Winter	34.7	0.0027	0.0006	1.7	-0.0250	-0.0015
Scenario A	Spring	9.1	0.0050	-0.0008	1.5	0.0038	-0.0006
	Summer	0.2	0.0055	-0.0134	6.7	0.0042	-0.0037
	Autumn	16.1	0.0053	0.0030	2.6	-0.0118	-0.0042
	Winter	10	0.0060	0.0048	1.2	-0.0143	0.0015
Scenario M2	Spring	0.7	0.0031	0.0083	0	-0.0054	-0.0098
	Summer	19.6	0.0036	-0.0014	4.6	-0.0064	-0.0117
	Autumn	28.5	0.0034	-0.0190	5.7	-0.0033	-0.0093
	Winter	25.9	0.0080	-0.0167	1.1	-0.0054	-0.0100
Scenario H	Spring	20.0	0.0039	-0.0011	10.0	-0.0058	-0.0019
	Summer	1.5	0.0022	-0.0059	10.0	-0.0068	-0.0034
	Autumn	29.8	0.0027	0.0065	0.9	-0.0150	-0.0050
	Winter	35.1	0.0053	-0.0068	5.8	-0.0045	-0.0048